

This is an Open Access document downloaded from ORCA, Cardiff University's institutional repository:<https://orca.cardiff.ac.uk/id/eprint/159147/>

This is the author's version of a work that was submitted to / accepted for publication.

Citation for final published version:

Luo, Qiqi, Yang, Xia, Hang, Jian, Fan, Xiaodan, Luo, Zhiwen , Gu, Zhongli and Ou, Cuiyun 2023. Influence of natural ventilation design on the dispersion of pathogen-laden droplets in a coach bus. *Science of the Total Environment* 885 , 163827. [10.1016/j.scitotenv.2023.163827](https://doi.org/10.1016/j.scitotenv.2023.163827)

Publishers page: <http://dx.doi.org/10.1016/j.scitotenv.2023.163827>

Please note:

Changes made as a result of publishing processes such as copy-editing, formatting and page numbers may not be reflected in this version. For the definitive version of this publication, please refer to the published source. You are advised to consult the publisher's version if you wish to cite this paper.

This version is being made available in accordance with publisher policies. See <http://orca.cf.ac.uk/policies.html> for usage policies. Copyright and moral rights for publications made available in ORCA are retained by the copyright holders.



## Journal Pre-proof

Influence of natural ventilation design on the dispersion of pathogen-laden droplets in a coach bus

Qiqi Luo, Xia Yang, Jian Hang, Xiaodan Fan, Zhiwen Luo, Zhongli Gu, Cuiyun Ou



PII: S0048-9697(23)02448-8

DOI: <https://doi.org/10.1016/j.scitotenv.2023.163827>

Reference: STOTEN 163827

To appear in: *Science of the Total Environment*

Received date: 8 February 2023

Revised date: 19 April 2023

Accepted date: 25 April 2023

Please cite this article as: Q. Luo, X. Yang, J. Hang, et al., Influence of natural ventilation design on the dispersion of pathogen-laden droplets in a coach bus, *Science of the Total Environment* (2023), <https://doi.org/10.1016/j.scitotenv.2023.163827>

This is a PDF file of an article that has undergone enhancements after acceptance, such as the addition of a cover page and metadata, and formatting for readability, but it is not yet the definitive version of record. This version will undergo additional copyediting, typesetting and review before it is published in its final form, but we are providing this version to give early visibility of the article. Please note that, during the production process, errors may be discovered which could affect the content, and all legal disclaimers that apply to the journal pertain.

© 2023 Published by Elsevier B.V.

To be submitted to Science of The Total Environment 2023

## **Influence of natural ventilation design on the dispersion of pathogen-laden droplets in a coach bus**

Qiqi Luo<sup>a,b#</sup>, Xia Yang<sup>c#</sup>, Jian Hang<sup>a,b</sup>, Xiaodan Fan<sup>a,b</sup>, Zhiwen Luo<sup>d</sup>, Zhongli Gu<sup>e</sup>,  
Cuiyun Ou<sup>a,b\*</sup>

<sup>a</sup>School of Atmospheric Sciences, Sun Yat-sen University, and Southern Marine Science and Engineering Guangdong Laboratory (Zhuhai), Zhuhai, P.R. China

<sup>b</sup>Key Laboratory of Tropical Atmosphere-Ocean System (Sun Yat-sen University), Ministry of Education, Zhuhai (519000), P.R. China

<sup>c</sup>Guangdong Province Engineering Laboratory for Air Pollution Control, Guangzhou, P.R. China

<sup>d</sup>Welsh School of Architecture, Cardiff University, UK

<sup>e</sup>Guangdong Fans-tech Agro Co., Ltd. China

Corresponding author: Cuiyun Ou:

Tel: +86-13487313916; E-mail address: oucuiyun@mail.sysu.edu.cn

First authors: Qiqi Luo, Xia Yang

## Abstract

Natural ventilation is an energy-efficient design approach to reduce infection risk (IR), but its optimized design in a coach bus environment is less studied. Based on a COVID-19 outbreak in a bus in Hunan, China, the indoor-outdoor coupled CFD modeling approach is adopted to comprehensively explore how optimized bus natural ventilation (e.g., opening/closing status of front/middle/rear windows (FW/MW/RW)) and ceiling wind catcher (WCH) affect the dispersion of pathogen-laden droplets (tracer gas, 5  $\mu\text{m}$ , 50  $\mu\text{m}$ ) and IR. Other key influential factors including bus speed, infector's location, and ambient temperature ( $T_{\text{ref}}$ ) are also considered. Buses have unique natural ventilation airflow patterns from bus rear to front, and air change rate per hour ( $ACH$ ) increases linearly with bus speed. When driving at 60 km/h,  $ACH$  is only 6.14  $\text{h}^{-1}$  and intake fraction of tracer gas ( $IF_g$ ) and 5  $\mu\text{m}$  droplets ( $IF_d$ ) are up to 3372 ppm and 1394 ppm with ventilation through leakages on skylights and no windows open. When FW and RW are both open,  $ACH$  increases by 43.5 times to 267.50  $\text{h}^{-1}$ , and  $IF_g$  and  $IF_d$  drop rapidly by 1-2 orders of magnitude compared to when no windows are open. Utilizing a wind catcher and opening front windows significantly increases  $ACH$  (up to 8.8 times) and reduces  $IF$  (5-30 times) compared to only opening front windows. When the infector locates at the bus front with FW open,  $IF_g$  and  $IF_d$  of all passengers are <10 ppm. More droplets suspend and further spread

in a higher  $T_{ref}$  environment. It is recommended to open two pairs of windows or open front windows and utilize the wind catcher to reduce IR in coach buses.

**Keywords:** droplet dispersion, window, infection risk, wind catcher, temperature, computational fluid dynamics simulation

Journal Pre-proof

Nomenclature			
$ACH$	Air change rate per hour	$N_t$	Total released droplet number
$C$	Concentration	PLD	Pathogen-laden droplets
$C_2H_6$	Ethane	$Q_p$	Tracer gas flow rate in passenger's nose
$C_c$	Cunningham slip correction factor	$Q_t$	Tracer gas flow rate in infector's mouth
CFD	Computational fluid dynamics	$Q_v$	Volumetric flow rate
$C_{i,\infty}$	Vapor concentration of bulk air	$R$	Correlation coefficient
$C_{i,s}$	Vapor concentration at droplet surface	$Re_p$	Reynolds number
COVID-19	Coronavirus disease 2019	$RH$	Relative humidity
$D$	Molecular diffusivity of mass	RNG	R-normalization group
$D_{i,m}$	Diffusion coefficient of vapor in bulk	RW	Rear windows
$d_p$	Initial droplet diameter	SARS-CoV-2	Severe acute respiratory syndrome coronavirus 2
$F_{a,i}$	Additional forces	$Sc$	Schmidt number
$FB$	Fraction bias	$t$	Time
$f_D$	Stoke's drag modification function	$T_a$	Ambient temperature
$F_{drag,i}$	Drag force	$U$	Stream-wise velocity
$F_{g,i}$	Gravity	$u^*$	Friction velocity
FW	Front windows	$u_{d,i}$	Velocity of droplet
$g_i$	Gravitational acceleration	$u_i$	Velocity of air
$H$	Height	$U_{ref}$	Reference velocity
$H_v$	Height of building	$Vol$	Volume
$IF$	Intake fraction	$\nu$	Kinematic viscosity
$IF_d$	Intake fraction of droplets	WCH	Wind catcher
$IF_g$	Intake fraction of tracer gas	$z_0$	Roughness height
IR	Infection risk	$\mu_t$	Turbulent viscosity
$k$	Turbulence kinetic energy	$\varepsilon$	Turbulent kinetic energy dissipation rate
$k_c$	Mass transfer coefficient	$\kappa$	Von Karman's constant
MW	Middle windows	$\lambda$	Molecular mean free path of air
$N_i$	Molar flux of vapor	$\rho$	Density of air
$NMSE$	Normalized mean square error	$\rho_d$	Density of droplets
$N_p$	Droplet number inhaled by passenger	$\tau$	Age of air
		$\tau_p$	Aerosol characteristic response time

## 1. Introduction

Several respiratory infectious diseases, including influenza, tuberculosis, and Middle East respiratory syndrome, have threatened global public health in the last few decades. To date, humanity around the world is still battling against the coronavirus disease 2019 (COVID-19) caused by severe acute respiratory syndrome coronavirus 2 (SARS-CoV-2) and its variants (Lu et al., 2020). Airborne transmission is one of the predominated spread routes for infectious diseases (Li, 2021; Mikszewski et al., 2022). Large amounts of pathogen-laden droplets (PLD) can be released by the infector during normal respiratory activities (e.g., breathing, speaking, and coughing), and remain suspended in the air for long periods and cause transmission (Wang et al., 2021a). Numerous studies have demonstrated that adequate ventilation can avoid PLD accumulation, thus reducing the spread of respiratory diseases (e.g., Ghoroghi et al., 2022; Shinohara et al., 2021, Yang et al., 2020). On the contrary, insufficient ventilation can lead to an extremely high probability of cross-infection in indoor environments (Qian et al., 2021).

As one of the most popular public transportation for suburban and intercity transportation, coach buses have high population density, complex and frequent population movements, and possibly inadequate ventilation, leading to probable high-risk indoor environments for the transmission of respiratory diseases. Therefore, it is worth studying the ventilation, expiratory droplet dispersion, and infection risk

control in coach buses. In general, there are two methods to simulate natural ventilation in enclosures with Computational Fluid Dynamics (CFD): coupled approach and decoupled approach. In a coupled method, both the outdoor and indoor environments are simulated in a single computational domain. For a decoupled approach, the case study employed a two-step calculation procedure, i.e., the outdoor flow simulation is first conducted for the bus as a sealed body to obtain the pressure on the boundary condition for the second-step indoor ventilation simulation. Although the decoupled approach is easier to model and generate grids, its accuracy is easily compromised and may introduce important errors (Ramponi and Blocken, 2012; van Hooff and Blocken, 2010). Therefore, the coupled approach is preferred for indoor natural ventilation studies and is adopted in this paper. Pichardo-Orta et al. (2022) utilized the coupled approach to investigate the natural ventilation under two kinds of open window configurations in a bus. They found that the outdoor air entered through the rear window and then moves forward, which was also confirmed in our previous study (Luo et al., 2022). This unique airflow makes the bus environment different from other buildings. However, most studies mainly focused on the natural ventilation in building environments, such as classrooms (Ding et al., 2022; Mirzaie et al., 2021), restaurants (Li et al., 2021; Liu et al., 2021), and hospital wards (Huang et al., 2022; Kong et al., 2021; Satheesan et al., 2020). Therefore, it is worthwhile to conduct a



comprehensive study on the impact of natural ventilation design strategies on PLD dispersion, and potential infection risk in the coach bus.

In order to conduct a comprehensive study on the bus's natural ventilation, expiratory droplet dispersion, and potential infection risk, we simulate a coach bus with the coupled approach, focusing on the effect of opening windows and wind catcher. The size data of the bus comes from the experiments of Ou et al. (2022). The wind catcher is a common and effective device for improving natural ventilation in buildings (Calautit et al., 2014; Liu et al., 2018), while no relevant research on buses. We consider the wind catcher on the coach bus ceiling to explore its effectiveness in improving natural ventilation. Moreover, the speed of the bus is another key factor to determine the pressure distribution on the exterior surface of the bus and subsequently influences the natural ventilation in the bus cabin (Mathai et al., 2021). Therefore, the role of bus speed (30 km/h, 60 km/h, and 90 km/h) on natural ventilation is also investigated in this paper. Duan et al. (2021) confirmed that the infector's location has an impact on the infection risk of passengers. In addition, the ambient temperature and relative humidity ( $RH$ ) can affect the evaporation rate of droplets, which in turn affects the droplet dispersion process (Ahmadzadeh and Shams, 2022; Yang et al., 2020). However, our previous study (Luo et al., 2022) found that  $RH$  has a limited impact on droplet dispersion in the coach bus due to the complex indoor environment (e.g., long and narrow cabin space, numerous seats, and passengers). Therefore,

whether the ambient temperature can obviously affect droplet dispersion in buses needs further study. Given all these considerations, this study will also consider and explore the influence of all the aforementioned factors on droplet dispersion and potential infection risk in a naturally-ventilated bus environment.

In this study, CFD simulations are adopted to explore the effect of open windows (six configurations of open window positions and sizes), bus speed (30 km/h, 60 km/h, and 90 km/h), infector's location (bus front, bus middle, and bus rear), ambient temperature and *RH* (11 °C and 27 °C, *RH* = 35%) on droplet transmission and the potential infection risk among passengers. Moreover, the wind catcher combined with the bus is also considered. The dispersion of exhaled droplets is simulated using tracer gas and liquid-solid mixture droplets with initial diameters of 5 μm and 50 μm. In addition, human body thermal planes are also considered. All the flow field parameters are shown in Table. 1, in addition, we considered different exhaled droplets (tracer gas, 5 μm droplets, and 50 μm droplets). Four factors made this study unique:

Firstly, we choose the coupled approach to simulate the effect of opening window positions and areas on the natural ventilation in the coach bus.

Secondly, we originally combine the wind catcher with the coach bus and quantify its effectiveness in improving natural ventilation.

Thirdly, various infector's locations and ambient temperatures are considered.

Fourthly, we quantitatively explore the potential infection risk of passengers of each case and give corresponding epidemic prevention suggestions based on the results.

## 2. Methodology

### 2.1 Physical model

To explore the effect of opening windows and the wind catcher on increasing natural ventilation and thereby reducing the potential infection risk of passengers, we utilize the coach bus which occurred the one-infecting-seven COVID-19 epidemic as the physical model in this paper. The target coach bus is a double-decker 48-seat bus with the passenger cabin on the upper deck and the driver zone on the lower deck with a dimension of 11.40 m × 2.50 m × 3.50 m (length × width × height). (Luo et al., 2022; Ou et al., 2022). As shown in Fig. 1(a), the cabin is fully occupied and three infector positions (in scarlet) are selected at the bus front, bus middle, and bus rear to explore the impact of the infector's location on the potential infection risk of other passengers. There are ring-shaped leakages on two skylights on the bus roof. The rear skylight can be turned into a wind catcher of size 1 m × 1 m × 0.4 m (length × width × height).

Three pairs of windows exist in the front/middle/rear lateral walls, which can open all (0.6 m × 0.8 m), open half (0.3 m × 0.8 m), or close all.

By using the coupled approach, the outdoor wind flow and indoor airflow are modeled simultaneously in the same computational domain, as presented in Fig. 1(b). The bus model is placed in a computational domain with sizes 130 m × 60 m × 23 m (length × width × height). The blockage ratio of the computational domain in this research is smaller than 1.37% to avoid blockage effects (Terminaga et al., 2008).

Fig. 1(c) depicts the grid arrangements of the model. Refined boundary layers are employed in places where the velocity gradient may be large: 0.005 m for the mouths and noses, 0.03 m around the manikin body, 0.01 m for the bus skylights, 0.05 m for the bus surfaces (Fig. 1c), and the maximum grid size is 1.5 m in the whole computational domain. The unstructured grid is used for the area around the coach bus and the structured grid is used for the external flow field. A total of 6,116,915 grids are generated and the grid independence has been validated in Luo et al. (2022).

## 2.2 Numerical simulation

In this study, the simulation of COVID-19 transmission is numerically calculated step by step. Firstly, the steady airflow field is solved by utilizing the RNG  $k-\varepsilon$  model. The RNG  $k-\varepsilon$  model has been verified to simulate airflows with considerable accuracy

and computing efficiency (Yakhot and Orszag, 1986; Yang et al., 2020). The second-order upwind scheme is applied to discretize all governing equations. The Boussinesq hypothesis is utilized to account for the effect of thermal buoyancy, in which air density is constant except for the vertical velocity-momentum equation.

After solving the steady airflow field, the dispersion of the tracer gas and the tracking of the droplets are simulated, respectively. Species transport model is adopted to calculate the tracer gas ( $C_2H_6$ ) dispersion and ambient relative humidity ( $RH = 35\%$ ).  $C_2H_6$  is selected as a tracer gas to represent the transport behavior of fine droplet nuclei ( $< 1 \mu m$ ), which has been confirmed in many studies (Liu et al., 2021; Villafruela et al., 2016; Yin et al., 2009), as well as in our previous study (Luo et al., 2022). The mass fraction of  $C_2H_6$  in the exhaled stream from the infector's mouth is 0.32, according to our previous studies (Luo et al., 2022; Ou et al., 2022).  $RH$  in the cabin is 35% when simulating droplet dispersion. Droplets are expelled from the mouth of the infector and tracked by discrete phase modeling.

The trajectories of PLD are evaluated by adopting Newton's second law in a Lagrangian framework (Mirzaie et al., 2021; Yang et al., 2022):

$$\frac{du_{d,i}}{dt} = F_{drag,i} + F_{g,i} + F_{a,i} \quad (1)$$

where  $u_{d,i}$  is droplet velocity in the  $i$  direction,  $F_{drag,i}$  is the drag force (Eq. (2)),  $F_{g,i}$  is the gravity (Eq. (3)),  $F_{a,i}$  is the additional forces for which we only considered

Brownian force and Saffman's lift force to account for the effects of Brownian motion and shear lift on a droplet (Yang et al., 2020; Zhang and Li, 2012).

$$F_{drag,i} = \frac{f_D}{\tau_p} (u_i - u_{d,i}) \quad (2)$$

$$F_{g,i} = \frac{g_i(\rho_d - \rho)}{\rho_d} \quad (3)$$

where  $f_D$  is the Stoke's drag modification function of large aerosol Reynolds number ( $Re_p$ ) (Eq. (4)),  $\tau_p$  is the aerosol characteristic response time (Eq. (5)),  $\rho_d$  is the density of droplet,  $u_i$  and  $\rho$  are the air's velocity and density, respectively.

$$f_D(Re_p) = 1 + 0.15 Re_p^{0.687} \quad (4)$$

$$\tau_p = \frac{\rho_d d_p^2 C_c}{18\mu_t} \quad (5)$$

where  $d_p$  is the droplet diameter,  $\mu_t$  is the turbulent viscosity, and  $C_c$  is the Cunningham correction to Stokes' drag law computed as:

$$C_c = 1 + \frac{2\lambda}{d_p} [1.257 + 0.4e^{-(1.1d_p/\lambda)}] \quad (6)$$

where  $\lambda$  is the molecular mean free path.

Our simulations consider the evaporation process of droplets with a solid-liquid ratio of 1:9, where the solid density is  $2170 \text{ kg/m}^3$  and the liquid density is  $998.2 \text{ kg/m}^3$  (Luo et al., 2022; Yang et al., 2020). The evaporation process of the liquid water in the droplet is related to the gradient of the vapor concentrations between the droplet surface and the surrounding air:

$$N_i = k_c(C_{i,s} - C_{i,\infty}) \quad (7)$$

$$Sh_{AB} = \frac{k_c d_p}{D_{i,m}} = 2.0 + 0.6 Re_p^{1/2} Sc^{1/3} \quad (8)$$

where  $N_i$  is the molar flux of vapor,  $C_{i,s}$  and  $C_{i,\infty}$  are the concentration of vapor at the droplet surface and the bulk, respectively.  $k_c$  is the mass transfer coefficient, which is calculated from the Sherwood number correlation (Eq. (8)).  $D_{i,m}$  is the diffusion coefficient of vapor in bulk.  $Sc$  is the Schmidt number which is defined as  $Sc = \frac{\nu}{D}$ , where  $\nu$  is the kinematic viscosity, and  $D$  is the molecular diffusivity of mass.

We adopt 5  $\mu\text{m}$  and 50  $\mu\text{m}$  droplets to explore the transmission process, in which 50  $\mu\text{m}$  droplets are simulated only when exploring the effect of temperature on droplet transmission. The droplet dispersion is simulated in the unsteady state. Single-diameter droplets are uniformly released from the infector's mouth at a rate of 10 droplets per time step ( $\Delta t = 0.1$  s) for 30 minutes, producing a total of 180,000 droplets. The initial velocity of the exhaled droplets is 1.5 m/s with an initial temperature of 32 °C (Luo et al., 2022). The following assumptions are adopted in simulations: (1) Droplet-airflow interaction is neglected as the concentration of droplets is low (Yang et al., 2020; Zhao et al., 2005); (2) There is no breakup or coagulation for the droplet deposition process (Satheesan et al., 2020; Yao and Liu, 2021); (3) The droplets are all in ideal sphere shape; (4) The breathing action of the infector is idealized as a uniform exhalation process with the temperature and velocity

of the exhaled airflow and droplets remaining constant (32 °C, 1.5 m/s), and other passengers are set to only have inhalation process (Liu et al., 2021; Luo et al., 2022).

### 2.3 Boundary conditions

The boundary conditions of CFD simulations are shown in Table A.1. At the domain inlet, the velocity and temperature are different with variable running conditions (8.33 m/s, 16.67 m/s, 25 m/s; 27 °C, 11 °C). Outflow boundary condition is adopted for the domain outlet, and symmetry condition is applied on the domain roof and lateral boundaries. For all wall treatments, no-slip wall boundary conditions are applied. The interior is selected as the boundary condition when the window is open, and the wall is utilized when it is closed. When the wind catcher is not in use, there is a skylight on the bus roof (Fig. 1(a)), and the side and top of the wind catcher adopt the interior as the boundary condition. When the wind catcher is used, the top and three side walls adopt the wall as the boundary condition, and the front and bottom (i.e., the bus roof) of the wind catcher are set as the interior. Note that leakages on two skylights are always kept open. A heat flux of 58 W/m<sup>2</sup> is set for each passenger to consider the effect of the human thermal plume in all cases (Tung et al., 2009). We assume that the infector exhales from the mouth steadily, and the rest passengers inhale through their noses.



Boundary conditions of droplet dispersion are set as the same as our previous study (Luo et al., 2022). The trap condition is applied at seats, human body surfaces, and floor, which means that droplets are trapped once they touch the objects, and the trajectory calculation is terminated. For the bus roof, vertical walls, and luggage racks, reflect condition was used due to gravity, which means that droplets bounced off the surfaces and continued to disperse. Escape condition is applied to the domain inlet, domain outlet, and noses of passengers (except the infector).

Ansys FLUENT is applied in numerical case studies. Convergence of simulations is obtained when the residuals for continuity equation, velocity components, energy, turbulence kinetic energy ( $k$ ), and turbulent kinetic energy dissipation rate ( $\epsilon$ ) are below  $10^{-4}$ ,  $10^{-6}$ ,  $10^{-8}$ ,  $10^{-5}$ , and,  $10^{-4}$ , respectively. We also monitor variables at specific points until they are stable, and check energy balance and mass balance to help determine the convergence. The CFD simulations in this study are completed on the Tianhe II supercomputer with the support of the National Supercomputer Center in Guangzhou.

## 2.4 Assessment indexes of natural ventilation and potential infection risk

### 2.4.1 Natural ventilation

The air change rate per hour (*ACH*) is widely adopted to evaluate indoor ventilation, which indicates the rate of the total indoor volume replaced by the fresh external air:

$$ACH = \frac{3600Q_v}{Vol} \quad (9)$$

where  $Q_v$  and  $Vol$  are the volumetric flow rate and the volume of the bus cabin, respectively. The volume of our bus cabin ( $Vol$ ) is 51.47 m<sup>3</sup>.

The local mean age of air is defined as the time of external air reaching an arbitrary point after entering the room, assuming that the external air is clean and its age is zero. A large age of air means that indoor ventilation is poor, and external fresh air takes a long time to arrive. The homogeneous tracer gas emission method is selected to calculate the age of air in this paper (Jin et al., 2016). A pollutant is released at a homogeneous rate ( $\dot{m} = 10^{-7} \text{ kg} \cdot \text{m}^{-3} \cdot \text{s}^{-1}$ ) in the bus cabin, and the age of air ( $\tau$ ) is proportional to the concentration obtained at the same point ( $C$ ):

$$\tau = \frac{C}{\dot{m}} \quad (10)$$

Note that the age of air mentioned below is the mean age of air in the bus cabin.

### 2.4.2 Potential infection risk

Intake fraction ( $IF$ ) is selected to measure the potential infection risk of passengers. Intake fraction of tracer gas ( $IF_g$ ) and droplets ( $IF_d$ ) are defined as (Liu et al., 2021; Yang et al., 2021):

$$IF_g = \frac{Q_p}{Q_t} \quad (11)$$

$$IF_d = \frac{N_p}{N_t} \quad (12)$$

where  $Q_p$  and  $Q_t$  are the flow rates of tracer gas in the passenger's nose and the infector's mouth, respectively.  $N_p$  is the number of droplets inhaled by the passenger and  $N_t$  is the total number of droplets released from the infector (180,000). The unit of  $IF_g$  and  $IF_d$  is ppm.

### 2.5 Validation of numerical modeling

The validation of indoor airflow, temperature, and particle dispersion has been done in our previous study (Luo et al., 2022), and the evaluation of tracer gas spread by the field experimental data can be found in Ou et al. (2022). In addition, the coupled indoor-outdoor model is validated by a wind tunnel experiment (Jiang et al., 2003). As shown in Fig. A.1(a), a cubic building model with a height of 2.5 m ( $H_v = 2.5$  m) is built and the scale ratio of the building model to the wind tunnel model is

10:1. There are two openings with a size of 1.25 m × 0.84 m in the middle of windward and leeward wall. The dimensions of the domain are the same as those in the simulation of Jiang et al., (2003). Two grid arrangements, a fine grid (0.05 m) and a coarse grid (0.1 m) (Fig. 2(b)), are considered for the building model. Two turbulence models, RNG  $k$ - $\varepsilon$  model and Standard  $k$ - $\varepsilon$  model, are performed for the numerical simulation.

Reynolds similarity is important to ensure accurate full scale airflow simulations. The reference Reynolds number is over 162,000 in the wind tunnel experiment, which is big enough to ensure Reynolds independence ( $>11,000$ ). The vertical profiles of the stream-wise velocity ( $U$ ) at the domain inlet,  $k$ , and  $\varepsilon$  are defined as:

$$U(z) = \frac{u^*}{\kappa} \ln\left(\frac{z}{z_0}\right) \quad (13)$$

$$k(z) = \frac{u^{*2}}{\sqrt{C_\mu}} \quad (14)$$

$$\varepsilon(z) = \frac{C_\mu^{3/4} k^{3/2}}{\kappa z} \quad (15)$$

where  $u^*$  is the friction velocity (= 1.068 m/s),  $\kappa$  is Von Karman's constant taken as 0.41,  $z_0$  is the roughness height (= 0.05 m), and  $C_\mu$  equals 0.09. All data are derived from wind tunnel tests and previous literature (Jiang et al., 2003; Jin et al., 2016).

Three lines are selected to compare the normalized velocity profiles ( $U_{ref} = 10$  m/s) of simulation results and wind tunnel data (Fig. A.1(b)). As depicted in Fig. A.1(c), the velocity profiles of simulation results show a good agreement with the

experimental data and all correlation coefficients  $> 0.9$ , which suggest the good performance of existing CFD methods in predicting coupled indoor-outdoor ventilation airflow. Moreover, simulation results are quantitatively evaluated on their accuracies by utilizing three validation metrics (Table A.2): correlation coefficient ( $R$ ), fractional bias ( $FB$ ), and normalized mean square error ( $NMSE$ ). The acceptance criteria are  $R > 0.8$ ,  $-0.3 < FB < 0.3$ , and  $NMSE < 1.5$ , respectively (Moonen and Allegrini, 2015). According to Table A.2, the fine grid with RNG  $k-\varepsilon$  model satisfies all validation metrics with exceptionally high  $R (> 0.9)$ , appropriate  $FB (< 0.3)$ , and low  $NMSE$  values ( $< 0.1$ ). Therefore, RNG  $k-\varepsilon$  model and fine grid are chosen to conduct CFD simulations in this study.

### 3. Results and discussion

The natural ventilation, dispersion of tracer gas and droplets, and potential infection risk are explored in three separate sections. Based on the results, corresponding suggestions and measures are provided to prevent the spread of COVID-19 in vehicles. Since the driver and passengers are located on different decks, the infector has limited influence on the driver, thus this paper mainly focuses on exploring the potential infection risk of passengers.

### 3.1 Natural ventilation

When the coach bus is running, the external airflow generates a pressure distribution over the bus's outdoor surfaces (Fig. A.2(a)). The area at the front of the bus outside is lower than the atmospheric pressure, while the area near the rear of the bus outside is higher than the atmospheric pressure, which is consistent with other studies (Li et al., 2015; Pichardo-Orta et al., 2022). Such pressure distribution leads to the unique airflow field in the cabin: the outdoor air enters the bus cabin from the rear openings and exits from the front openings, i.e., the indoor main airflow is from the rear to the front (Fig. A.2(b)). Moreover, as the windows open, the airflow velocity in the bus cabin becomes larger and the human body thermal plume will be disrupted (Fig. A.3). In this section, the bus travels at a speed of 60 km/h, except for section 3.1.3 where 30 km/h and 90 km/h are adopted to explore the effect of bus speed on natural ventilation.

#### 3.1.1 Effect of opening windows on natural ventilation

The natural ventilation under various open window configurations is listed in Table 2 and the special distribution of the age of air is depicted in Fig. A.4. Note that no wind catcher is used in this section. As expected,  $ACH$  is small (only  $6.14 \text{ h}^{-1}$ ) when no windows are open and only ventilation through two leakages (Case 1). When the front windows are open (Case 2),  $ACH$  increases 5 times to  $31.4 \text{ h}^{-1}$ . It is worth

noting that if two pairs of windows are open (Case 3, 4), the natural ventilation will increase significantly:  $ACH$  is 22.6-43.5 times more than that of Case 1. Especially,  $ACH$  can reach  $267.5 \text{ h}^{-1}$  and the age of air reduces to 7.33 s when opening the front and rear windows (Case 4). The reason for the remarkable increase in natural ventilation can be explained by the pumping effect (Li et al., 2015). When the windows are opened at locations with a large pressure difference between indoor and outdoor (Case 3 and Case 4 in this study), the indoor air will flow like a "pump", and the ventilation will be greatly enhanced (Matose et al., 2019; Pichardo-Orta et al., 2022). Therefore, it is beneficial to open the front and rear windows, which can provide sufficient natural ventilation in the vehicle. In addition, it is interesting to find that  $ACH$  in Case 5 (all windows half open,  $146.37 \text{ h}^{-1}$ ) is almost half of  $ACH$  in Case 6 (all windows open,  $293.36 \text{ h}^{-1}$ ). It indicates that the ventilation rate is essentially proportional to the open window area, which is also confirmed in Shinohara et al., 2021.

### 3.1.2 Effect of wind catcher on natural ventilation

Wind catcher is often applied to improve the natural ventilation of buildings (Calautit et al., 2014; Liu et al., 2018). We skillfully combine it with the coach bus, and demonstrate its effectiveness on improving ventilation in this section (Fig. 2(a)). When no windows are open (Case 1, 7),  $ACH$  increases from  $6.14 \text{ h}^{-1}$  to  $12.68 \text{ h}^{-1}$ , and the age of air decreases from 469.03 s to 127.26 s with the adoption of the wind

catcher. When the front windows are open (Case 8),  $ACH$  can increase to  $277.70 \text{ h}^{-1}$ , which is 8.8 times larger than without the wind catcher (Case 2). Meanwhile, the age of air is about 16.6 parts of that without the wind catcher. Montazeri and Montazeri (2018) found that opening windows could improve the ventilation efficiency of the wind catcher in a single-zone isolated building, especially opening windows far from the wind catcher. It indicates that a wind catcher combined with opening windows can be more effective in improving natural ventilation inside the bus. When all windows are open with the wind catcher (Case 9),  $ACH$  reaches  $450.23 \text{ h}^{-1}$  and the age of air is only 6.21 s. Moreover, the installation of a wind catcher can not only significantly enhance natural ventilation, but also substantially improve the thermal comfort of passengers (Fig. A.5).

### 3.1.3 Effect of bus speed on natural ventilation

To make the change in ventilation more visible, we explore the effect of bus speed on ventilation when all windows are open. Fig. 2(b) displays the variation of  $ACH$  and the age of air with bus speed when all windows are opened (Case 6). When the speed increases from 30 km/h to 90 km/h, the age of air in the carriage decreases from 21.49 s to 4.54 s. In addition,  $ACH$  is positively correlated with bus speed. When the bus speed is 90 km/h,  $ACH$  is up to  $448.86 \text{ h}^{-1}$ . When the bus speed is 30 km/h,  $ACH$  is only  $146.07 \text{ h}^{-1}$ . Therefore, the speed of the vehicle is an important factor affecting the natural ventilation in the cabin. The slower the vehicle speed, the lower



the *ACH*, the older the age of air, the greater the potential risk of passenger infection (Li et al., 2017). Mathai et al. (2022) recommended that when a car was stuck in a traffic jam, it may be beneficial to open the front windows, and turn on the air conditioner to the maximum while opening the mechanical ventilation to effectively remove the aerosols released by people. In short, we need to pay special attention to ventilation when driving at low speeds, which requires opening more windows and even utilizing mechanical ventilation to ensure adequate natural ventilation.

### 3.2 Dispersion of tracer gas and droplets

We utilize tracer gas and solid-liquid mixed droplets to explore the dispersion process of human exhaled droplets. Tracer gas is adopted to simulate the spread of fine droplets ( $< 1 \mu\text{m}$ ) (Luo et al., 2022). Solid-liquid mixed droplets of  $5 \mu\text{m}$  and  $50 \mu\text{m}$  are selected in this study, where  $50 \mu\text{m}$  droplets are simulated only when exploring the effect of temperature on droplet transport (section 3.2.4). *RH* is 35% in the cabin for all cases. After complete evaporation, the nuclei diameters of droplets with initial diameters of  $5 \mu\text{m}$  and  $50 \mu\text{m}$  are  $1.82 \mu\text{m}$  and  $18.25 \mu\text{m}$ , respectively. All cases in this section are at a bus speed of  $60 \text{ km/h}$ , the infector is located at the bus rear (12D) except in section 3.2.3, and the initial droplet diameter is  $5 \mu\text{m}$  with an ambient temperature of  $27 \text{ }^\circ\text{C}$  except in section 3.2.4.

### 3.2.1 Effect of opening windows on dispersion

As depicted in Fig. 3, when no windows are open, the tracer gas concentration is generally above 250 ppm and can be up to 359.65 ppm near the infector. Droplets are concentrated in the bus rear due to the weak airflow in the cabin. With the opening of front windows, the tracer gas concentration in the bus front reduces 1-3 times to 80.40-135.31 ppm. However, there is still a relatively high tracer gas concentration in the bus rear, especially in the row where the infector is located and in the three rows in front him where can be above 278.09 ppm. In addition, more droplets can move forward with the airflow, but only few of them can be discharged out of the cabin. Since the ventilation increases greatly with the opening of front and rear windows, the tracer gas concentration in the cabin is only 3.20-5.16 ppm at the bus front and 25.89-50 ppm at the bus rear, which is 7-50 times lower than when no windows are opened. Moreover, the droplets in the cabin are greatly reduced. In Fig. 3, we can find that the birth time of droplets is generally large (in red) for Case 4 and Case 6, which means that the droplets will quickly spread forward and be discharged out of the bus once they are exhaled by the infector. However, it is somewhat surprising that when all windows are open, the tracer gas concentration and droplets is slightly higher on the infector's side (columns C and D, the seat arrangement is displayed in Fig. 1(a)) (4.47 ppm-14.16 ppm) compared to when the front and rear windows are open (3.20-5.16 ppm). Similarly, droplets are moving forward more and spread less in other

directions (e.g., spread vertically and to the other side of the infector) when all windows are open. The reason can be traced back to the strong forward airflow, which drives the tracer gas and droplets to spread forward, thus we can find a lower concentration of tracer gas (1.31 ppm) and fewer droplets on the other side of the infector (columns A, B, and E).

### 3.2.2 Effect of wind catcher on dispersion

Fig. 4 compares the average concentration of tracer gas and the number of suspended droplets in the bus cabin with and without the wind catcher. In all configurations, the average tracer gas concentration and suspended droplet number decline to varying degrees with the position of the wind catcher. When no windows are opened, with the opening of the wind catcher, the average tracer gas concentration of the cabin reduces from 258.53 ppm to 56.78 ppm (drops to one-fifth) and the suspended droplet number reduces from 4870 to 3079. The most noticeable decline appears when opening the front windows. Compared with the situation without the wind catcher, the tracer gas concentration using the wind catcher decreased by more than 18 times (from 108.99 ppm to 5.8 ppm), and the number of suspended droplets decreased by more than 4 times (from 3145 to 761). When all windows are open, the average tracer gas concentration reduces from 4.81 ppm to 2.11 ppm and the suspended droplet number reduces from 400 to 342. These data reaffirm the previous

conclusion in section 3.1.2 that the wind catcher works more effectively when combined with opening windows.

### 3.2.3 Effect of infector location on dispersion

The location of the infector is an important factor to influence the exhaled droplet dispersion in the bus. As the natural ventilation is sufficient when two pairs of windows are open, exhaled droplets will discharge rapidly regardless of where the infector is located. Thus, we adopt the configuration when the front windows are open to investigate the droplet dispersion as the infector gradually approaches the window (Fig. 5). Since the airflow in the bus cabin is from the rear to the front, the tracer gas and droplets are mainly transported forward. As the infected person moves forward near the windows, their transmission range will be shortened. When the infector is located at the bus rear (Fig. 3), the tracer gas and droplets can be dispersed in the whole cabin, especially concentrated in the bus rear. While the infector is in the bus middle (Fig. 5), there are only few droplets at the bus rear, and the tracer gas concentration is only 4.40 ppm. Droplets and tracer gas are mainly concentrated in three rows in front of the infector and the row where the infector is located. When the infector is located at the bus front, most exhaled matter can be discharged quickly from windows near the infector, so there are only few droplets in the whole cabin, and the tracer gas concentration is only 0.77 ppm except the area near the infector. Zhang et al. (2021) have mentioned that when the infector is at the bus front, the risk of

passengers is lower than when the infector is in the bus middle of an opening-window bus. Moreover, Yao and Liu (2021) have recommended opening a window in front of the infector, which is beneficial to remove droplets in the bus. Namely, the infector or potentially infected person should sit in the front row and open the nearby windows to reduce the potential infection risk of others in a natural ventilation bus.

### 3.2.4 Effect of ambient temperature on dispersion

The rising ambient temperature can accelerate the evaporation process, because the surrounding air will provide latent heat for droplets to promote their evaporation (Pal et al., 2021). As  $5\ \mu\text{m}$  droplets will evaporate completely into droplet nuclei in 0.1 s, we select  $50\ \mu\text{m}$  droplets to simulate in this section. To make the temperature influence droplet diffusion more obvious, we chose the case of no windows open, which is also more consistent with the actual situation of closing all windows when the temperature is low. As presented in Fig. 6(a), when the ambient temperature is  $27\ ^\circ\text{C}$ , it takes only 1.5 s for  $50\ \mu\text{m}$  droplets to evaporate completely into  $18.25\ \mu\text{m}$  droplet nuclei, while it takes 2.2 s for the ambient temperature of  $11\ ^\circ\text{C}$ . Consequently, under a higher ambient temperature, the droplet evaporation time is shorter, so the smaller droplets can spread more forward and upward (Fig. 6(b)). Ahmadzadeh et al. (2022) have investigated the transmission of coughing droplets in a train through CFD simulations. They found that high temperature was an ideal condition for droplet evaporation, thus more droplets were suspended in the air at higher temperatures.

Nonetheless, it is also mentioned in Wang et al. (2021b) that large droplets (e.g., 100  $\mu\text{m}$ ) take a much longer time to evaporate and their transmission may be more affected by the temperature. However, for small droplets or when the ambient velocity field is relatively large, the effect of temperature may be limited.

### 3.3 Potential infection risk of passengers

Intake fraction of tracer gas ( $IF_g$ ) and droplets ( $IF_d$ ) are utilized to measure the potential infection risk of passengers in this section. Passengers without data or with data of zero indicate that they do not inhale droplets exhaled by the infector. The exposure time for all cases is 30 min.

#### 3.3.1 Effect of opening windows on potential infection risk

As the natural ventilation is poor when no windows are open,  $IF_g$  of all passengers is above 1300 ppm (Fig. 7), and can even reach 3235.49 ppm for the passenger in the infector's adjacent seat (12C). As weak airflow makes most droplets concentrated in the bus rear (as depicted in Fig. 3), high  $IF_d$  appears at the bus rear and the highest  $IF_d$  is 1394.44 ppm for 12C.

With the opening of the front windows,  $IF_g$  for passengers in rows 1-6 substantially decreases to less than 500 ppm, but it remains high for passengers around the infector (around 1000 ppm). We note that  $IF_d$  of passengers in the three

rows in front of the infector (rows 9-11 of columns C and D) generally increases instead, because the enhanced airflow delivers more droplets forward. Nevertheless, for most of the remaining passengers,  $IF_d$  is reduced to varying degrees (e.g., from 1394.44 ppm to 650.00 ppm for 12C).

When both front and rear windows are open,  $IF_g$  is less than 80 ppm for all passengers except for 12B and 12C. The highest  $IF_g$  still occurs at 12C, but its value is only 170.95 ppm, which is nearly 19 times lower than the situation when no windows are open. This remarkable reduction is also presented in the  $IF_d$ , most passengers do not inhale droplets exhaled by the infector ( $IF_d = 0$ ), and the maximum  $IF_d$  is 72.22 at 12C.

When all windows are open, passengers in columns A, B, and E (the other side of the infector) all have a low  $IF_g$  (< 21.79 ppm). However, for passengers in columns C and D (the same side of the infector), compared with the situation when the front and middle windows are open,  $IF_g$  changes little and even increases slightly. Similarly, most passengers in columns A, B, and E do not inhale PLD, while most passengers in columns C and D have small  $IF_d$  (< 80 ppm). This is due to the strong forward airflow, making the tracer gas and droplets mainly spread forward, which is consistent with the finding in Fig. 3. Edwards et al. (2021) also confirmed that when all the windows were opened in a bus, the droplet count in the cabin decreased significantly, but droplets would transport over a longer distance in the direction of the airflow. This

means that when there is a strong airflow in the vehicle, we should pay attention not to sit downwind of the dominant airflow.

### 3.3.2 Effect of wind catcher on potential infection risk

It has been verified in section 3.1.2 that the wind catcher has a great benefit to enhance natural ventilation. Especially when the front windows are open,  $ACH$  can increase nearly 9 times compared with the situation without the wind catcher. Therefore, the wind catcher can greatly affect the potential infection risk of passengers. Fig. 8 compares the potential infection risk of passengers when the front windows are open with and without the wind catcher. We can find that  $IF_g$  of columns A, B, and E considerably reduces 9-39 times and all of them are below 50 ppm when the wind catcher is open. Moreover,  $IF_g$  of passengers in columns C and D also declines significantly, especially in the latter rows (rows 10-13) of columns C and D where the decline is quite notable (over 24 times). This phenomenon also applies to droplets. After using the wind catcher, the  $IF_d$  of most passengers in columns A and B is zero, which means that passengers will not inhale PLD. Meanwhile,  $IF_g$  of passengers at 10C-13C and 10D-13D also decreases markedly (over 5 times).

### 3.3.3 Effect of infector's location on potential infection risk

Fig. 9 depicts the potential infection risk of passengers when the infector is located at different positions with the opening of front windows. When the infector



sits at the bus rear (Fig. 7),  $IF_g$  of all passengers is above 223.54 ppm, and it is more than 500 ppm for that of passengers at the rear of the bus. In addition, most passengers have inhaled PLD with relatively high  $IF_d$  at the bus rear. When the infector is in the middle of the cabin (Fig. 9),  $IF_g$  and  $IF_d$  of the passengers behind him dropped significantly. For the passengers in rows 9 to 13,  $IF_g$  is basically below 80 ppm and none of them inhaled droplets. However, the potential infection risk of passengers in rows 3-6 of columns C and D is significantly higher, with  $IF_g$  greater than 597 ppm and  $IF_d$  generally greater than 200 ppm. When the infector is in the front of the cabin,  $IF_g$  of all passengers is less than 40 ppm, and most passengers do not inhale droplets. In all cases, we can find that no matter where the infector is located, the seat adjacent to the infector and the three rows in front of the infector are high-risk areas, which is also confirmed in Pichardo-Orta et al. (2022) and Yao and Liu (2021). In other words, the passengers behind the infector, especially the passengers in the rear three rows, have a relatively low potential risk of infection, which is a relatively safe place.

### 3.3.4 Effect of ambient temperature on potential infection risk

In this section, we select 50  $\mu\text{m}$  droplets to calculate passengers' potential infection risk. Droplets will evaporate slowly at low ambient temperature, so droplets can spread a short distance due to gravity. As depicted in Fig. 10, when the ambient temperature is 11  $^{\circ}\text{C}$ , the farthest position for passengers to inhale 50  $\mu\text{m}$  droplets is

the sixth row (6B). At 27 °C, even the first-row passenger (1B) can inhale PLD. Namely, compared with 11 °C, more droplets spread forward at 27 °C, resulting in more passengers inhaling PLD. Moreover, as the ambient temperature increases,  $IF_g$  of passengers basically increases slightly. Under these two temperatures, the seat (12C) next to the infector has the highest  $IF_g$ , which is 1261.11 ppm and 1950.00 ppm at 11 °C and 27 °C, respectively. Temperature can affect the viral activity in droplets, and thereby impact the potential infection risk, which is not considered in this paper. This is one of the limitations of this study and also one of our future studies.

### 3.4 Recommendations for natural ventilation and disease prevention

It is generally recommended to increase ventilation in closed public transport as a preventive measure (World Health Organization, 2021), and its effectiveness has been confirmed in many studies (Bosch and Moreno, 2021; Mesgarpour et al., 2021; Vlachá et al., 2021). Since there is no public transport ventilation guide, it is recommended to follow the building ventilation guide. The Chinese standard is at least 30 m<sup>3</sup>/h per person (NHC, 2022). Fig. 11 describes the fresh air rate per person in different configurations.

Obviously, if there are no windows opened in the bus, the fresh air rate per person cannot reach the standard of 30 m<sup>3</sup>/h per person (Fig. 11(a)). When the front

windows are opened, the fresh air rate is  $34.39 \text{ m}^3/\text{h}$  per person, which just reaches the minimum standard when the bus speed is  $60 \text{ km/h}$ . In fact, when the vehicle is in a traffic jam or waiting for traffic lights, it is difficult to maintain a speed of  $60 \text{ km/h}$  or higher at all times. In addition, according to the 30-minute potential infection risk in Section 3.3, when the infector is in the middle or rear of the bus, the seat next to the infector and the passengers three rows in front of the infector still have a relatively high risk ( $IF_g > 590 \text{ ppm}$ ). Therefore, only opening front windows may not provide adequate natural ventilation for passengers. Opening two pairs of windows is an effective way to increase natural ventilation. When two or more pairs of windows are opened, even if all the windows are half open, the ventilation will greatly exceed the minimum indoor ventilation standard 6-10 times. Compared with the configuration without opening the window when the front and rear windows are opened,  $IF_g$  decreases 18 times, and nearly half of passengers do not inhale PLD ( $IF_d = 0$ ). In order to fully rely on the natural ventilation of windows, we need to open two or more pairs of windows, especially front and rear windows, to bring sufficient ventilation for passengers. When it is inconvenient to open windows in extreme weather, it is necessary to increase the fresh air rate of mechanical ventilation to ensure that passengers have adequate ventilation.

As one of the common devices to improve the natural ventilation of buildings, the wind catcher can also play a good role when combined with the coach bus,

especially when cooperating with windows. If only a wind catcher and leakages are used for ventilation, although the fresh air rate ( $13.89 \text{ m}^3/\text{h}$  per person) is doubled compared with that without the wind catcher ( $6.72 \text{ m}^3/\text{h}$  per person), it still cannot meet the minimum indoor standard (Fig. 11(a)-(b)). However, when both the wind catcher and front windows are open, the natural ventilation (which hardly meets the minimum standard when without the wind catcher) soars to  $304.11 \text{ m}^3/\text{h}$  per person, which is 10 times the minimum indoor ventilation standard. In terms of potential infection risk, when the wind catcher and front window are both opened,  $IF_g$  is reduced by 8-30 times compared with only opening the front windows.  $IF_d$  of the three rows of passengers next to and in front of the infector is reduced by at least 5 times, and the  $IF_d$  of the other passengers is almost zero. In addition, whether in winter or summer or even in weather conditions where windows are not suitable for opening (such as rainy days), the wind catcher can always improve the thermal comfort of passengers. (Fig. A.5). In summary, the adoption of the wind catcher can not only improve natural ventilation, but also ensure the thermal comfort of passengers. Hence, it is recommended to install a wind catcher for the bus, so that even if only a pair of windows are opened, the natural ventilation in the cabin can be greatly improved, hence reducing the potential infection risk of passengers.

Bus speed is an important factor affecting the natural ventilation in the bus cabin.

Fig. 11(c) depicts that the fresh air rate of passengers decreases rapidly as the bus

slows down. Therefore, we need to pay special attention to ventilation when vehicles drive slowly or stuck in traffic. The open window configurations that can provide sufficient ventilation when driving at high speed may be no longer suitable for driving at low speed. Especially when the vehicle is stationary, there is very little ventilation in the vehicle. Ou et al. (2022) measured the natural ventilation in a stationary bus and  $ACH$  is only  $0.62 \text{ h}^{-1}$ , that is,  $0.79 \text{ m}^3/\text{h}$  per person which is far less than the indoor ventilation standard. For a stationary vehicle, the 30-min exposure potential infection risk can be up to 15.29% (Luo et al., 2022), so in this case, mechanical ventilation is needed to increase the fresh air rate.

In almost all cases, we can find that the passenger next to the infector has the highest potential infection risk. Since the airflow in the cabin is from the rear to the front of the bus only relying on natural ventilation, the three rows in front of the infector also have a relatively great potential infection risk. Therefore, passengers should pay attention to avoid these high-risk positions when taking seats. However, in real life, we often cannot identify who is infected, so it is difficult to determine which seats are more dangerous. Nevertheless, no matter where the infector is, there is a high risk of being on the same side as the infector as well as downwind. Therefore, it is recommended that passengers avoid sitting on the same side. Even if sitting on the same side, passengers should be separated by at least three rows. When we are diagnosed infectors or possible infectors, we should take a seat at bus front with a

mask and open nearby windows. For healthy passengers, we should attempt to sit at the bus rear. In the case of good weather conditions, we can choose to open two or more pairs of windows, so that no matter where the infector is seated will be able to quickly discharge the droplets out of the cabin.

#### 4. Limitations and future research

Several limitations of the current study should be acknowledged. Different respiratory activities, such as breathing, talking, coughing, sneezing, etc., will produce droplets with different initial diameters (Clarke et al., 2009; Xu et al., 2015), but we only consider the diffusion process of droplets with small initial diameters ( $\leq 5 \mu\text{m}$ ) in the present study. In the future, we will consider the authentic droplet diameter distribution generated by human respiration, that is simultaneously releasing droplets with multiple initial diameters. The temperature and ambient relative humidity will affect the survival rates of infectious viruses in the droplets and thus the potential infection risk (Riddeil et al., 2020). It is worth investigating the effect of temperature and  $RH$  on virus survival rate and droplet transmission process. Furthermore, the steady RANS method utilized in this paper uses time-averaged treatment to simplify the unsteady Navier-Stokes equations governing fluid flow. Our future study will adopt unsteady computational methods, such as large eddy simulations, which could

give a more accurate assessment of droplet dispersion. Moreover, the steady state was adopted to simulate the tracer gas dispersion, which ignored the tracer gas diffusion process. In future studies, we will use unsteady simulations to consider the influence of tracer gas diffusion processes. This study finds that opening the window can quickly drive PLD out of the bus, which gives us inspiration. When it is inappropriate to open windows for a long time, we may take intermittent window opening to reduce the potential infection risk of passengers. For example, after driving for ten minutes without opening any windows, the concentration of PLD in the cabin will be very high. If two pairs of windows are opened at this time, the concentration in the cabin will reduce quickly, and how long to open the windows properly is a question that needs to be explored. Nowadays, we are studying how long it takes a closed vehicle to open windows for ventilation, and how to change the window opening strategy when the vehicle speed changes. In addition, we will also further explore the effect of vehicle speed on ventilation under different window opening conditions.

## 5. Conclusion

By performing CFD simulations, the effects of various open window configurations, the wind catcher, and bus speeds on bus natural ventilation are investigated. We also quantify the potential infection risk of each passenger under different natural ventilation conditions, three specific infector's locations, and ambient

temperature by adopting tracer gas and droplets (initial diameters of 5  $\mu\text{m}$  and 50  $\mu\text{m}$ ).

Key conclusions are summarized as follows:

1. Due to the positive pressure at the bus rear surface and the negative pressure at the front when the bus moves, the external airflow enters the bus from the rear openings and leaves from the front openings, thus forming a rear-to-front airflow in the cabin.
2. At the bus speed of 60 km/h, when there are no windows open and only leakages on two skylights for ventilation,  $ACH$  is only  $6.14\text{ h}^{-1}$ , resulting in a high potential infection risk of passengers with  $IF_g$  and  $IF_d$  up to 3235.49 ppm and 1394.44 ppm, respectively. Opening the front and rear windows can significantly increase  $ACH$  to  $267.50\text{ h}^{-1}$ , resulting in 7-50 times lower  $IF_g$  (7.26-170.95 ppm), than when no windows are opened, and nearly half of the passengers do not inhale droplets.
3. Installing a wind catcher in the coach bus ceiling can both greatly improve natural ventilation and passenger thermal comfort. When the wind catcher and front windows are opened with a bus speed of 60 km/h,  $ACH$  is  $277.70\text{ h}^{-1}$ , which is 8.8 times higher than when the wind catcher is not used. Moreover,



$IF_g$  decreases 8-30 times to 2.22 ppm-240.42 ppm and  $IF_d$  of passengers in three rows in front of the infector decreases more than 5 times ( $< 34$  ppm).

4. When all windows are open (at the front, middle and rear of the bus),  $ACH$  and bus speed are linearly related within the range of 30 km/h to 90 km/h: when the bus speed is 30 km/h, 60 km/h, and 90 km/h,  $ACH$  is  $146.07 \text{ h}^{-1}$ ,  $293.36 \text{ h}^{-1}$ , and  $448.86 \text{ h}^{-1}$ , respectively.
5. When front windows are opened, the diffusion range of tracer gas and droplets is smaller as the infector's location moves forward. Wherever the infector is, the passengers in the three rows in front of the infector have a relatively high potential infection risk. When the infector is located at the bus front,  $IF_g$  and  $IF_d$  of all passengers are less than 10 ppm.
6. The  $50 \mu\text{m}$  droplets take 2.2 s to completely evaporate into droplet nuclei at an ambient temperature of  $11 \text{ }^\circ\text{C}$ , and 1.5 s at  $27 \text{ }^\circ\text{C}$ . When the ambient temperature is  $11 \text{ }^\circ\text{C}$ ,  $50 \mu\text{m}$  droplets can only spread to the sixth row and be inhaled, while at  $27 \text{ }^\circ\text{C}$ , the first-row passenger can inhale droplets.

Based on the results, the practical implications of this study are summarized as follows: (1) When the bus is running, at least two pairs of windows, especially the front and rear windows, should be opened to ensure sufficient ventilation for passengers. (2) It is recommended to install a wind catcher on public vehicles and

use it with a pair of windows to supply extensive natural ventilation. (3) When the vehicle is moving slowly or stationary, all windows should be opened, and mechanical ventilation should be adopted to provide fresh air. (4) During the period of epidemic traffic control, passengers should avoid sitting on the same side of the cabin and be separated by at least three rows. (5) When we are diagnosed infectors or possibly infected people, we should take a seat in the front rows and open nearby windows. Healthy people are recommended to sit in the bus rear.

## **Acknowledgments**

This work was supported by Guangdong Major Project of Basic and Applied Basic Research [2021B0301030007, 2020B0301030004]; R&D Plan Project in Key Fields of Guangdong Province [212020012620600004]; and the National Natural Science Foundation of China [grant numbers 42175095, 42005069]. The support from UK GCRF Rapid Response Grant on ‘Transmission of SARS-CoV-2 virus in crowded indoor environment’, and the Innovation Group Project of the Southern Marine Science and Engineering Guangdong Laboratory (Zhuhai) [No. 311020001] are also gratefully acknowledged.

## References

1. Ahmadzadeh, M., Shams, M. (2022). Multi-objective performance assessment of HVAC systems and physical barriers on COVID-19 infection transmission in a high-speed train. *Journal of Building Engineering*, 53, 104544. <https://doi.org/10.1016/j.jobbe.2022.104544>
2. Bosch, A., Moreno, N. (2021). Tracing surface and airborne SARS-CoV-2 RNA inside public buses and subway trains. *Environment International*, 147, 106326. <https://doi.org/10.1016/j.envint.2020.106326>
3. Calautit, J., Connor, D., Hughes, B. (2014). Determining the optimum spacing and arrangement for commercial wind towers for ventilation performance. *Building and Environment*, 82, 274–287. <https://doi.org/10.1016/j.buildenv.2014.08.024>
4. Chao, C., Wan, M., Morawska, L., Johnson, G., Ristovski, Z., Hargreaves, M., Mengersen, K., Corbett, S., Li, Y., Xie, X., Katoshevski, D. (2009). Characterization of expiration air jets and droplet size distributions immediately at the mouth opening. *Journal of Aerosol Science*, 40(2), 122–133. <https://doi.org/10.1016/j.jaerosci.2008.10.003>
5. Ding, E., Zhang, D., Bluyssen, P. (2022). Ventilation regimes of school classrooms against airborne transmission of infectious respiratory droplets: A review. *Building and Environment*, 207, 108484. <https://doi.org/10.1016/j.buildenv.2021.108484>
6. Duan, W., Mei, F., Li, J., Liu, Z., Jia, M., Hou, S. (2021). Spatial distribution of exhalation droplets in the bus in different seasons. *Aerosol and Air Quality Research*, 21(8), 200478. <https://doi.org/10.4209/aaqr.200478>
7. Edwards, N., Widrick, R., Wilmes, J., Breisch, B., Gerschevske, M., Sullivan, J., Potember, R., Espinoza-Calvio, A. (2021). Reducing COVID-19 airborne transmission risks on public transportation buses: an empirical study on aerosol dispersion and control. *Aerosol Science and Technology*, 55(12), 1378–1397. <https://doi.org/10.1080/02786826.2021.1966376>
8. Ghoroghi, A., Rezgui, Y., Wallace, R. (2022). Impact of ventilation and avoidance measures on SARS-CoV-2 risk of infection in public indoor environments. *Science of the Total Environment*, 838, 156518. <https://doi.org/10.1016/j.scitotenv.2022.156518>
9. Huang, W., Wang, K., Hung, C., Chow, K., Tsang, D., Lai, R., Xu, R., Yeoh, E., Chen, C., Ho, K. (2022). Evaluation of SARS-CoV-2 transmission in COVID-19 isolation wards: On-site sampling and numerical analysis. *Journal of Hazardous Materials*, 436, 129152. <https://doi.org/10.1016/j.jhazmat.2022.129152>

10. Jiang, Y., Alexander, D., Jenkins, H., Arthur, R., Chen, Q. (2003). Natural ventilation in buildings: Measurement in a wind tunnel and numerical simulation with large-eddy simulation. *Journal of Wind Engineering and Industrial Aerodynamics*, 91(3), 331–353. [https://doi.org/10.1016/S0167-6105\(02\)00380-X](https://doi.org/10.1016/S0167-6105(02)00380-X)
11. Jin, R., Hang, J., Liu, S., Wei, J., Liu, Y., Xie, J., Sandberg, M. (2016). Numerical investigation of wind-driven natural ventilation performance in a multi-storey hospital by coupling indoor and outdoor airflow. *Indoor and Built Environment*, 25(8), 1226–1247. <https://doi.org/10.1177/1420326X15595689>
12. Kong, X., Guo, C., Lin, Z., Duan, S., He, J., Ren, Y., Ren, J. (2021). Experimental study on the control effect of different ventilation systems on fine particles in a simulated hospital ward. *Sustainable Cities and Society*, 73, 103102. <https://doi.org/10.1016/j.scs.2021.103102>
13. Li, F., Lee, E., Liu, J., Zhu, Y. (2015). Predicting self-pollution inside school buses using a CFD and multi-zone coupled model. *Atmospheric Environment*, 107, 16–23. <https://doi.org/10.1016/j.atmosenv.2015.02.024>
14. Li, F., Lee, E., Zhou, B., Liu, J., Zhu, Y. (2017). Effects of the window openings on the micro-environmental condition in a school bus. *Atmospheric Environment*, 167, 434–443. <https://doi.org/10.1016/j.atmosenv.2017.08.053>
15. Li, Y. (2021). Hypothesis: SARS-CoV-2 transmission is predominated by the short-range airborne route and exacerbated by poor ventilation. *Indoor Air*, 31(4), 921–925. <https://doi.org/10.1111/ina.12837>
16. Li, Y., Qian, H., Hang, J., Chen, X., Cheng, P., Ling, H., Wang, S., Liang, P., Li, J., Xiao, S., Wei, J., Liu, L., Cowling, B., Kang, M. (2021). Probable airborne transmission of SARS-CoV-2 in a poorly ventilated restaurant. *Building and Environment*, 196, 107788. <https://doi.org/10.1016/j.buildenv.2021.107788>
17. Liu, S., Luo, Z., Zhang, K., Hang, J. (2018). Natural ventilation of a small-scale road tunnel by wind catchers: A CFD simulation study. *Atmosphere*, 9(10), 411. <https://doi.org/10.3390/atmos9100411>
18. Liu, Z., Li, R., Wu, Y., Ju, R., Gao, N. (2021). Numerical study on the effect of diner divider on the airborne transmission of diseases in canteens. *Energy and Buildings*, 248, 111171. <https://doi.org/10.1016/j.enbuild.2021.111171>
19. Lu, R., Zhao, X., Li, J., Niu, P., Yang, B., Wu, H., Wang, W., Song, H., Huang, B., Zhu, N., Bi, Y., Ma, X., Zhan, F., Wang, L., Hu, T., Zhou, H., Hu, Z., Zhou, W., Zhao, L., Tan, W. (2020). Genomic characterisation and epidemiology of 2019 novel coronavirus: Implications for virus origins and receptor binding. *The Lancet*, 395(10224), 565–574. [https://doi.org/10.1016/S0140-6736\(20\)30251-8](https://doi.org/10.1016/S0140-6736(20)30251-8)

20. Luo, Q., Ou, C., Hang, J., Luo, Z., Yang, H., Yang, X., Zhang, X., Li, Y., Fan, X. (2022). Role of pathogen-laden expiratory droplet dispersion and natural ventilation explaining a COVID-19 outbreak in a coach bus. *Building and Environment*, 220, 109160. <https://doi.org/10.1016/j.buildenv.2022.109160>
21. Mathai, V., Das, A., Bailey, J. A., Breuer, K. (2021). Airflows inside passenger cars and implications for airborne disease transmission. *Science Advances*, 7(1), eabe0166. <https://doi.org/10.1126/sciadv.abe0166>
22. Mathai, V., Das, A., Breuer, K. (2022). Aerosol transmission in passenger car cabins: Effects of ventilation configuration and driving speed. *Physics of Fluids*, 34(2), 1–10. <https://doi.org/10.1063/5.0079555>
23. Matose, M., Poluta, M., Douglas, T. (2019). Natural ventilation as a means of airborne tuberculosis infection control in minibus taxis. *South African Journal of Science*, 115, 1–4. <https://doi.org/10.17159/sajs.2019/5737>
24. Mesgarpour, M., Abad, J., Alizadeh, R., Wongwises, S., Doranehgard, M., Ghaderi, S., Karimi, N. (2021). Prediction of the spread of Corona-virus carrying droplets in a bus - A computational based artificial intelligence approach. *Journal of Hazardous Materials*, 413, 125358. <https://doi.org/10.1016/j.jhazmat.2021.125358>
25. Mirzaie, M., Lakzian, E., Khar, A., Warkiani, M., Mahian, O., Ahmadi, G. (2021). COVID-19 spread in a classroom equipped with partition – A CFD approach. *Journal of Hazardous Materials*, 420, 126587. <https://doi.org/10.1016/j.jhazmat.2021.126587>
26. Mikszewski, A., Stabile, L., Buonanno, G., Morawska, L. (2022). Increased close proximity airborne transmission of the SARS-CoV-2 Delta variant. *Science of the Total Environment*, 816, 151499. <https://doi.org/10.1016/j.scitotenv.2021.151499>
27. Montazeri, H., Montazeri, F. (2018). CFD simulation of cross-ventilation in buildings using rooftop wind-catchers: Impact of outlet openings. *Renewable Energy*, 118, 502–520. <https://doi.org/10.1016/j.renene.2017.11.032>
28. Moonen, P., Allegrini, J. (2015). Employing statistical model emulation as a surrogate for CFD. *Environmental Modelling and Software*, 72, 77–91. <https://doi.org/10.1016/j.envsoft.2015.06.007>
29. National Health Commission (NHC). (2022). Standards for indoor air quality. GB/T 18883-2022. Accessed 11 July 2022.
30. Ou, C., Hu, S., Luo, K., Yang, H., Hang, J., Cheng, P., Hai, Z., Xiao, S., Qian, H., Xiao, S., Jing, X., Xie, Z., Ling, H., Liu, L., Gao, L., Deng, Q., Cowling, B., Li, Y. (2021). Insufficient ventilation led to a probable long-range airborne transmission of SARS-CoV-2 on two buses. *Building and Environment*, 207, 108414. <https://doi.org/10.1016/j.buildenv.2021.108414>

31. Pal, R., Sarkar, S., Mukhopadhyay, A. (2021). Influence of ambient conditions on evaporation and transport of respiratory droplets in indoor environment. *International Communications in Heat and Mass Transfer*, 129, 105750. <https://doi.org/10.1016/j.icheatmasstransfer.2021.105750>
32. Pichardo-Orta, F., Patiño-Luna, O., Vélez-Cordero, J. (2022). A frontal air intake may improve the natural ventilation in urban buses. *Scientific Reports*, 12(1), 21256. <https://doi.org/10.21203/rs.3.rs-1308008/v1>
33. Qian, H., Miao, T., Liu, L., Zheng, X., Luo, D., Li, Y. (2021). Indoor transmission of SARS-CoV-2. *Indoor Air*, 31(3), 639–645. <https://doi.org/10.1111/ina.12766>
34. Ramponi, R., Blocken, B. (2012). CFD simulation of cross-ventilation for a generic isolated building: Impact of computational parameters. *Building and Environment*, 53, 34–48. <https://doi.org/10.1016/j.buildenv.2012.01.004>
35. Riddell, S., Goldie, S., Hill, A., Eagles, D., Brown, T. (2020). The effect of temperature on persistence of SARS-CoV-2 on common surfaces. *Virology Journal*, 17(1), 1–7. <https://doi.org/10.1186/s12935-020-01418-7>
36. Satheesan, M., Mui, K., Wong, C. (2020). A numerical study of ventilation strategies for infection risk mitigation in general inpatient wards. *Building Simulation*, 13(4), 887–896. <https://doi.org/10.1007/s12273-020-0623-4>
37. Shinohara, N., Sakaguchi, J., Kim, H., Kagi, N., Tatsu, K., Mano, H., Iwasaki, Y., Naito, W. (2021). Survey of air exchange rates and evaluation of airborne infection risk of COVID-19 on commuter trains. *Environment International*, 157, 106774. <https://doi.org/10.1016/j.envint.2021.106774>
38. Tominaga, Y., Mochida, A., Yoshie, R., Kataoka, H., Nozu, T., Yoshikawa, M., Shirasawa, T. (2008). AIJ guidelines for practical applications of CFD to pedestrian wind environment around buildings. *Journal of Wind Engineering and Industrial Aerodynamics*, 96(10–11), 1749–1761. <https://doi.org/10.1016/j.jweia.2008.02.058>
39. Tung, Y. C., Shih, Y. C., Hu, S. C. (2009). Numerical study on the dispersion of airborne contaminants from an isolation room in the case of door opening. *Applied Thermal Engineering*, 29(8–9), 1544–1551. <https://doi.org/10.1016/j.applthermaleng.2008.07.009>
40. van Hooff, T., Blocken, B. (2010). Coupled urban wind flow and indoor natural ventilation modelling on a high-resolution grid: A case study for the Amsterdam ArenA stadium. *Environmental Modelling and Software*, 25(1), 51–65. <https://doi.org/10.1016/j.envsoft.2009.07.008>
41. Villafruela, J., Olmedo, I., San José, J. (2016). Influence of human breathing modes on airborne cross infection risk. *Building and Environment*, 106, 340–351. <https://doi.org/10.1016/j.buildenv.2016.07.005>

42. Vlachá, V., Feketea, G., Petropoulou, A., Trancá, S. (2021). The Significance of Duration of Exposure and Circulation of Fresh Air in SARS-CoV-2 Transmission Among Healthcare Workers. *Frontiers in Medicine*, 8, 1–7. <https://doi.org/10.3389/fmed.2021.664297>
43. Wang, C., Prather, K., Sznitman, J., Jimenez, J., Lakdawala, S., Tufekci, Z., Marr, L. (2021a). Airborne transmission of respiratory viruses. *Science*, 272. <https://doi.org/10.1126/science.abd9149>
44. Wang, J., Alipour, M., Soligo, G., Roccon, A., De Paoli, M., Picano, F., Soldati, A. (2021b). Short-range exposure to airborne virus transmission and current guidelines. *Proceedings of the National Academy of Sciences of the United States of America*, 118, 37. <https://doi.org/10.1073/pnas.2105279118>
45. World Health Organization. (2021). Coronavirus disease (COVID-19): Ventilation and air conditioning. Accessed 23 December 2021. <https://www.who.int/news-room/questions-and-answers/item/coronavirus-disease-covid-19-ventilation-and-air-conditioning#>
46. Xu, C., Nielsen, P., Gong, G., Liu, L., Jensen, R. (2015). Measuring the exhaled breath of a manikin and human subjects. *Indoor Air*, 25(2), 188–197. <https://doi.org/10.1111/ina.12129>
47. Yakhot, V., Orszag, S. (1986). Renormalization group analysis of turbulence. I. Basic theory. *Journal of Scientific Computing*, 1(1), 3–51. <https://doi.org/10.1007/BF01061452>
48. Yang, X., Ou, C., Yang, H., Liu, L., Song, T., Kang, M., Lin, H., Hang, J. (2020). Transmission of pathogen-laden expiratory droplets in a coach bus. *Journal of Hazardous Materials*, 397, 122609. <https://doi.org/10.1016/j.jhazmat.2020.122609>
49. Yang, X., Yang, H., Ou, C., Luo, Z., Hang, J. (2021). Airborne transmission of pathogen-laden expiratory droplets in open outdoor space. *Science of the Total Environment*, 773, 145537. <https://doi.org/10.1016/j.scitotenv.2021.145537>
50. Yang, X., Wang, Y., Tian, L., Su, C., Chen, Z., Huang, Y. (2022). Effects of purifiers on the airborne transmission of droplets inside a bus. *Physics of Fluids*, 34(1), 1–15. <https://doi.org/10.1063/5.0081230>
51. Yao, F., Liu, X. (2021). The effect of opening window position on aerosol transmission in an enclosed bus under windless environment. *Physics of Fluids*, 33, 123301. <https://doi.org/10.1063/5.0073171>
52. Yin, Y., Xu, W., Gupta, J., Guity, A., Marmion, P., Manning, A., Gulick, B., Zhang, X., Chen, Q. (2009). Experimental study on displacement and mixing ventilation systems for a patient ward. *HVAC and Research*, 15(6), 1175–1191. <https://doi.org/10.1080/10789669.2009.10390885>

53. Zhang, L., Li, Y. (2012). Dispersion of coughed droplets in a fully-occupied high-speed rail cabin. *Building and Environment*, 47(1), 58–66. <https://doi.org/10.1016/j.buildenv.2011.03.015>

54. Zhang, Z., Han, T., Yoo, K., Capecelatro, J., Boehman, A., Maki, K. (2021). Disease transmission through expiratory aerosols on an urban bus. *Physics of Fluids*, 33(1), 1–16. <https://doi.org/10.1063/5.0037452>

55. Zhao, B., Zhang, Z., Li, X. (2005). Numerical study of the transport of droplets or particles generated by respiratory system indoors. *Building and Environment*, 40(8), 1032–1039. <https://doi.org/10.1016/j.buildenv.2004.09.018>

Journal Pre-proof



**CRedit author contribution statement**

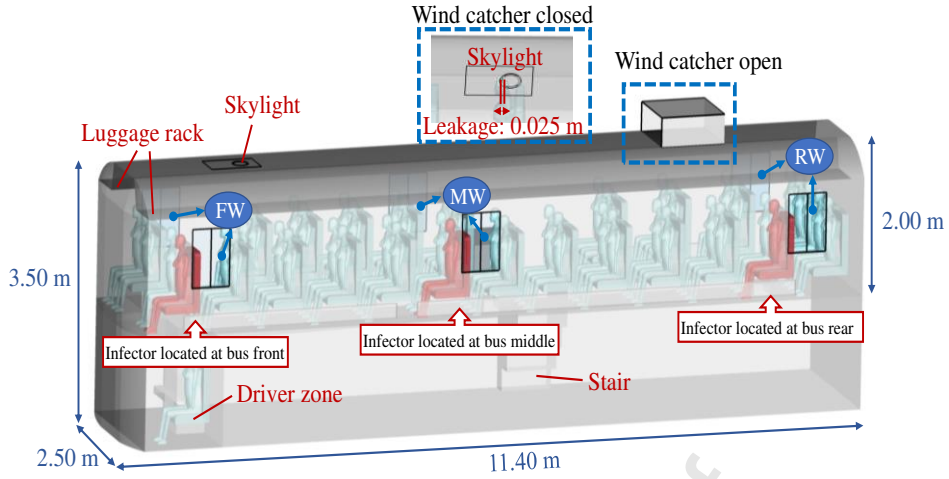
**Qiqi Luo:** Conceptualization, Data curation, Formal analysis, Methodology, Software, Visualization, Writing - original draft, Writing – review & editing. **Xia Yang:** Methodology, Data curation, Formal analysis, Methodology, Software, Writing – review & editing. **Jian Hang:** Conceptualization, Funding acquisition, Resources, Supervision, Writing – review & editing. **Xiaodan Fan:** Data curation, Writing – review & editing. **Zhiwen Luo:** Funding acquisition, Writing – review & editing. **Zhongli Gu:** Formal analysis, Software. **Cuiyun Ou:** Conceptualization, Formal analysis, Supervision, Resources, Project administration, Writing – review & editing.

**Declaration of interests**

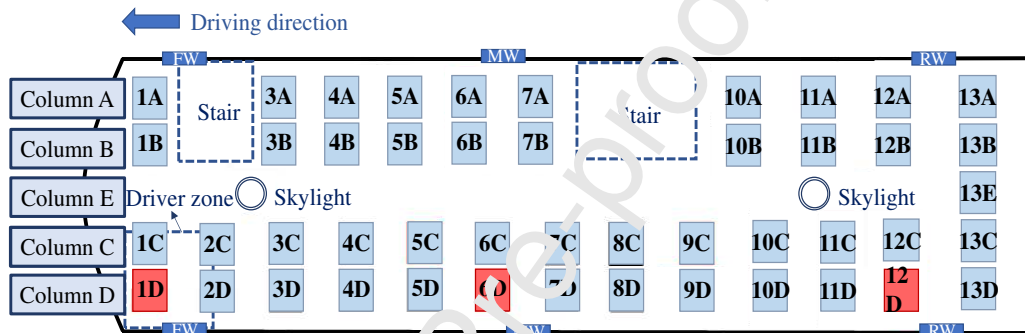
The authors declare that they have no known competing financial interests or personal relationships that could have appeared to influence the work reported in this paper.

The authors declare the following financial interests/personal relationships which may be considered as potential competing interests:

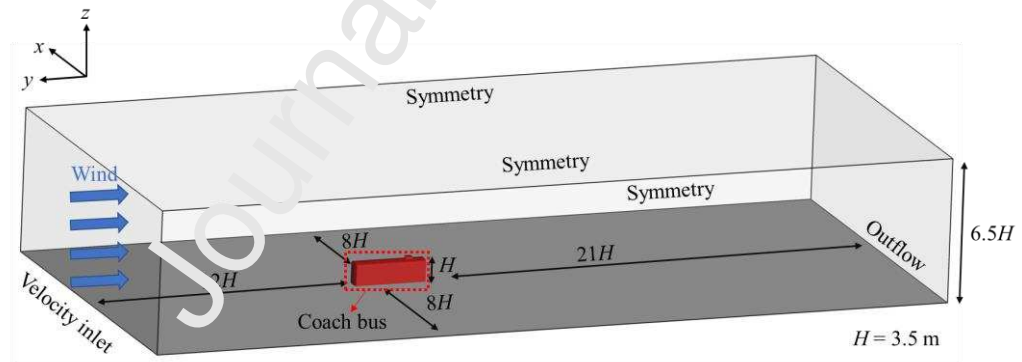
Journal Pre-proof



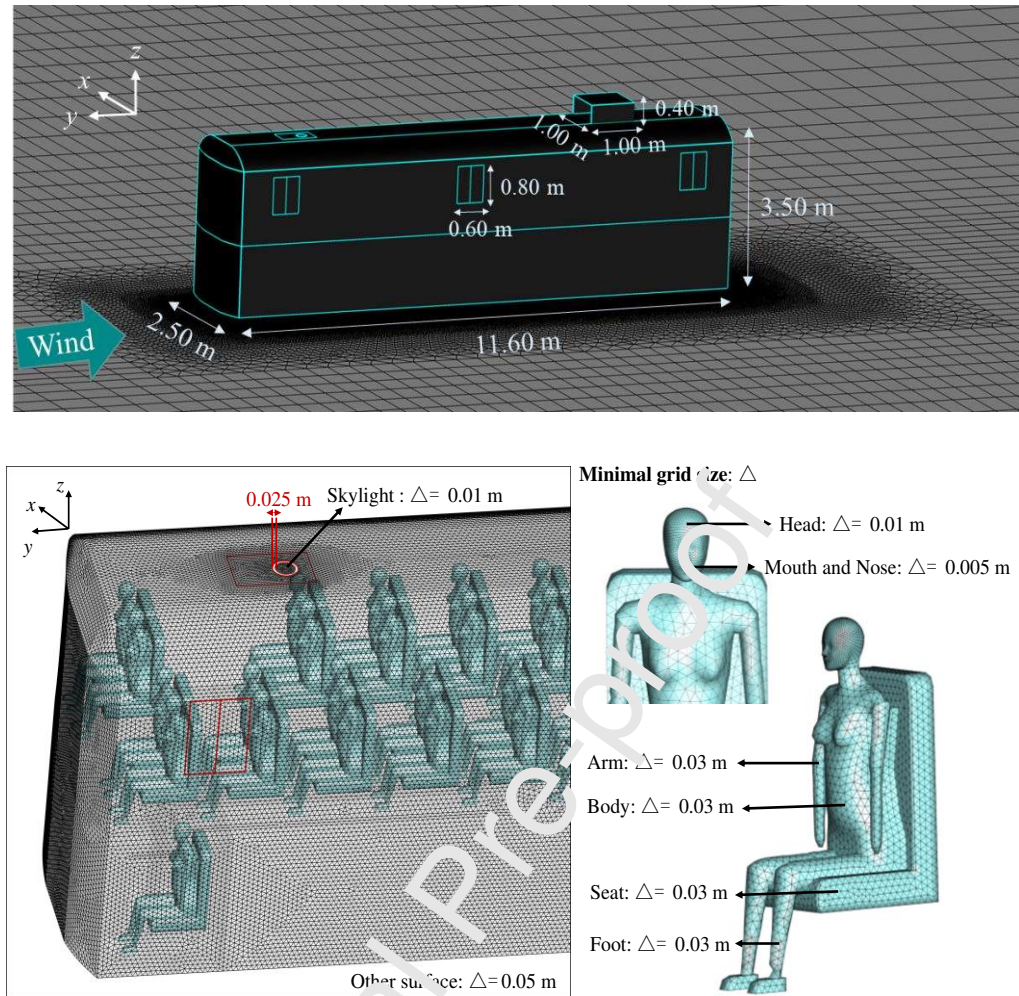
Note: 'FW' means 'front windows' 'MW' means 'middle windows' 'RW' means 'rear windows'



(a)

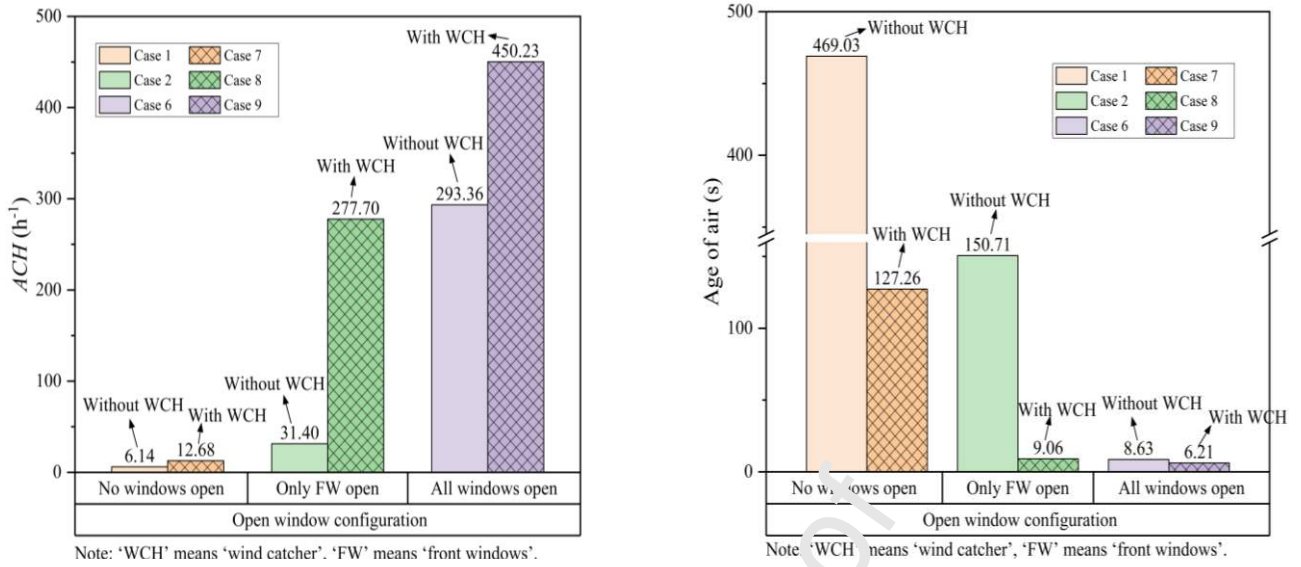


(b)

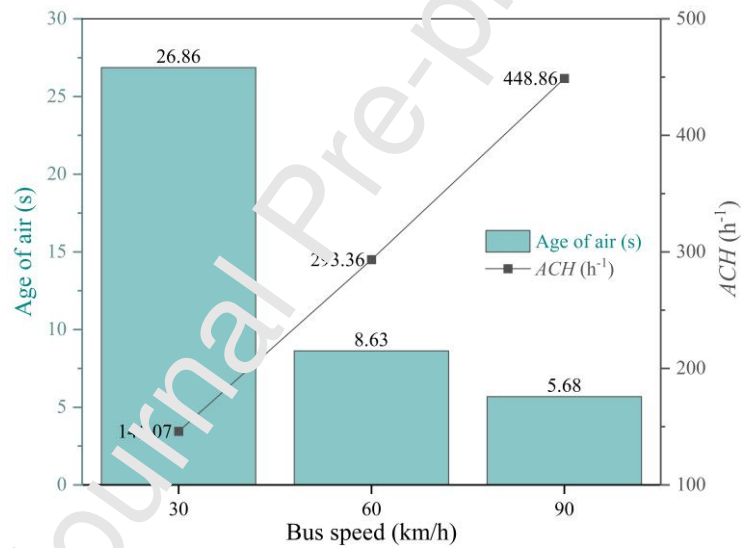


(c)

Fig. 1 (a) Description of computational domain and boundary conditions; (b) bus dimensions and seat arrangement; (c) grid arrangements of the computational domain.



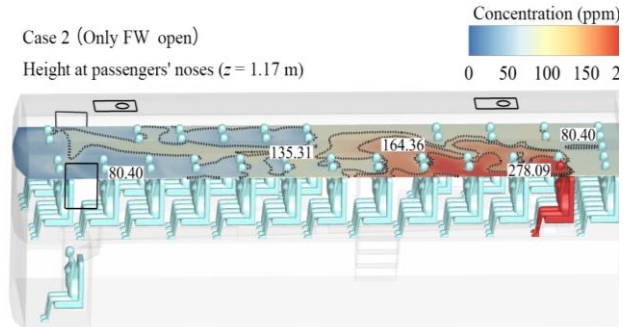
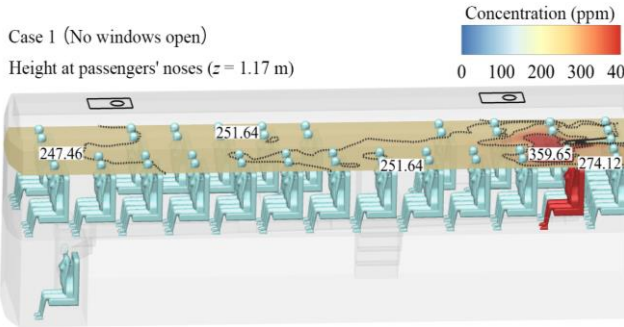
(a)



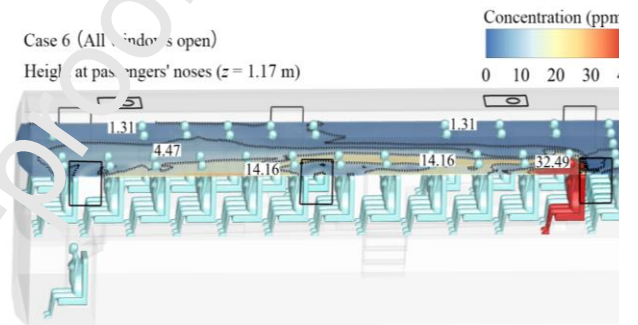
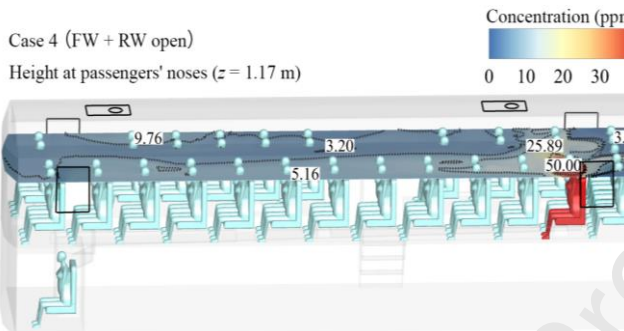
(b)

Fig. 2 (a) Comparison of ACH and age of air with and without wind catcher when bus is driving at 60 km/h; (b) change of ACH and age of air with various bus speeds when all windows are open.

Concentration field of tracer gas

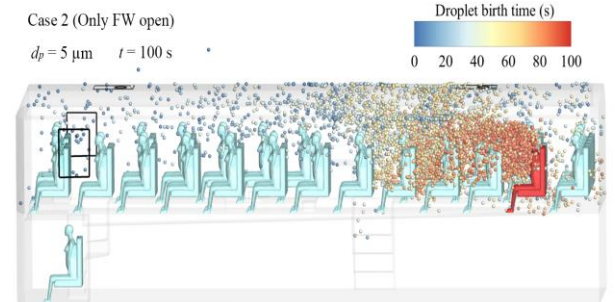
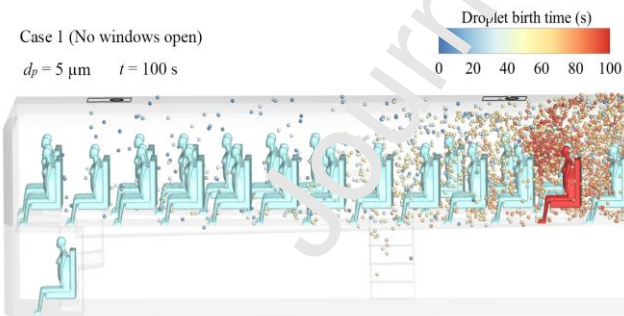


Note: 'FW' means 'front windows' .



Note: 'FW' means 'front windows' , 'RW' means 'rear windows' .

Spatial distribution of droplets



Note: 'FW' means 'front windows' .



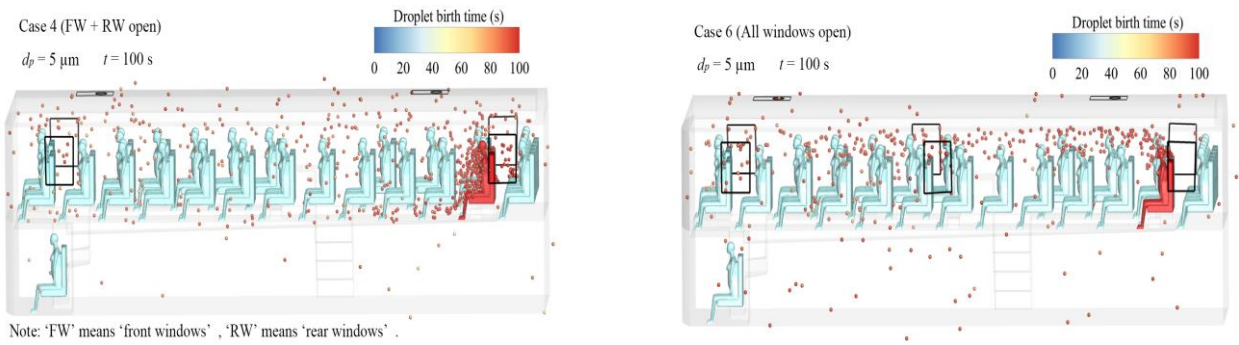
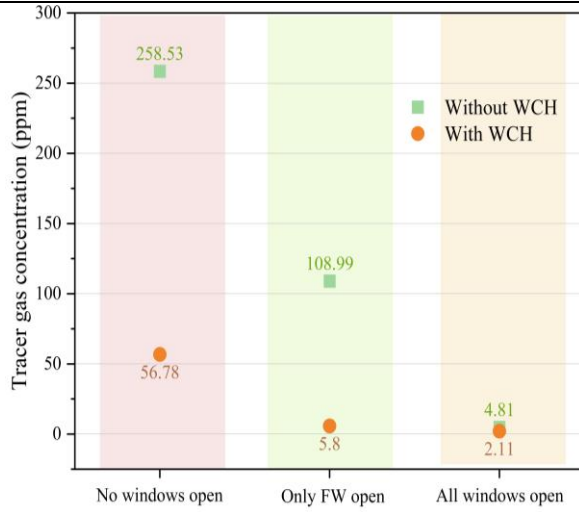


Fig. 3 Distribution field of tracer gas concentration and droplets under various open window configurations. (Bus speed = 60 km/h, ambient temperature = 27 °C,  $d_p = 5 \mu\text{m}$ )

Journal Pre-proof

Average tracer gas concentration in cabin



Number of suspended droplets in cabin

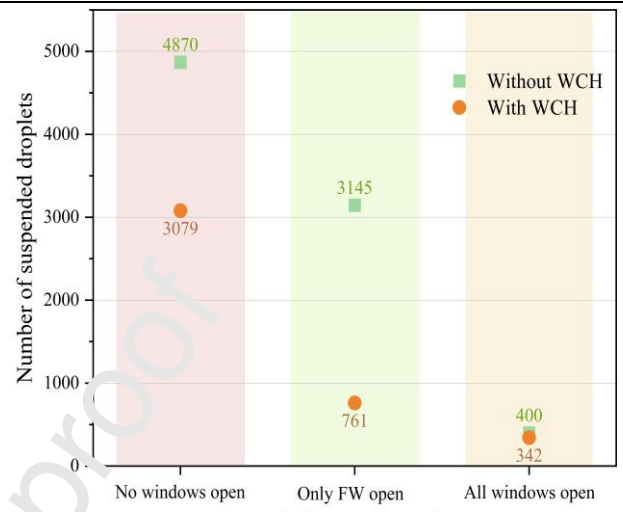
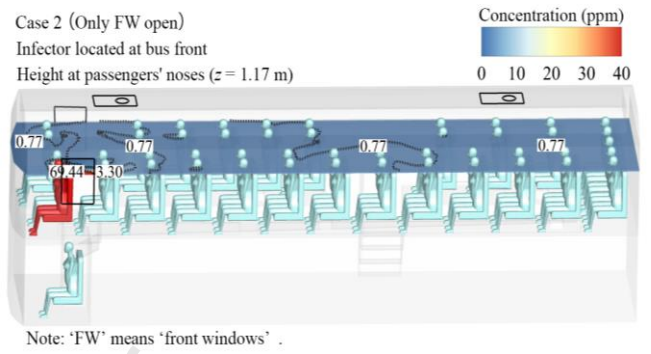
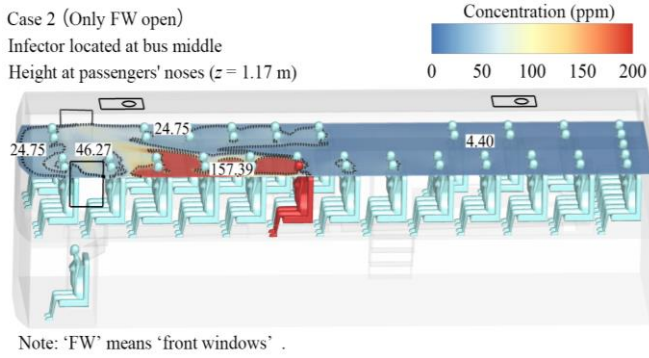


Fig. 4 Comparison of average tracer gas concentration and suspended droplet number in cabin with and without wind catcher. (Bus speed = 60 km/h, ambient temperature = 27 °C,  $d_p = 5 \mu\text{m}$ )



Concentration field of tracer gas



Spatial distribution of droplets

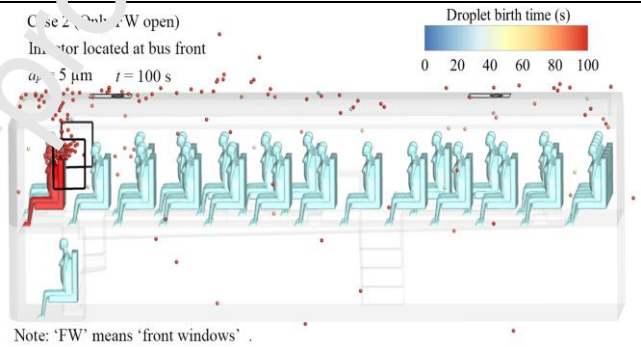
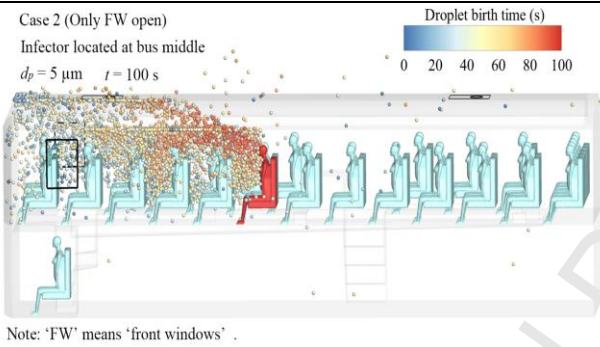
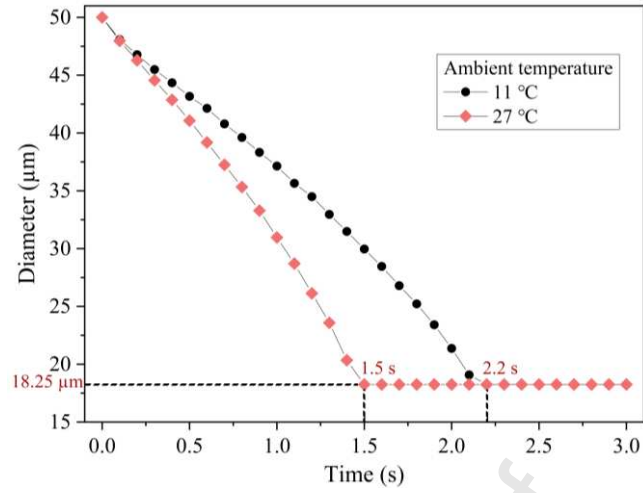
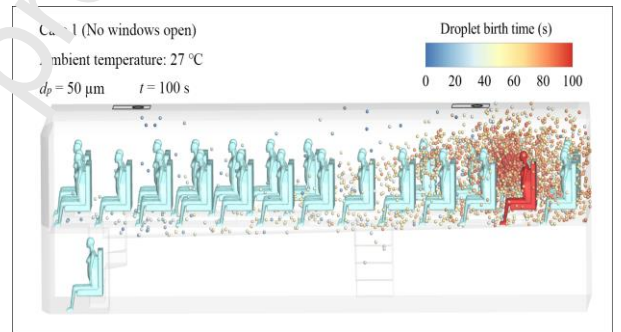
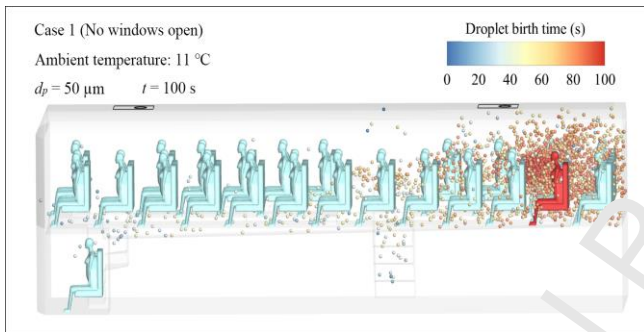


Fig. 5 Tracer gas concentration and droplet distribution under various infector locations when only front windows are open. (Bus speed = 60 km/h, ambient temperature = 27 °C,  $d_p = 5 \mu\text{m}$ )



(a)

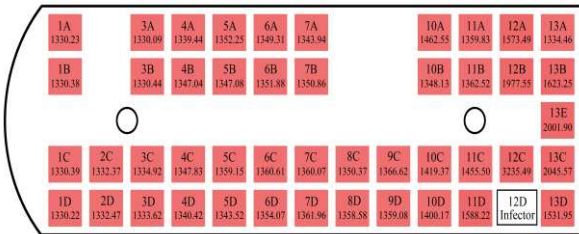


(b)

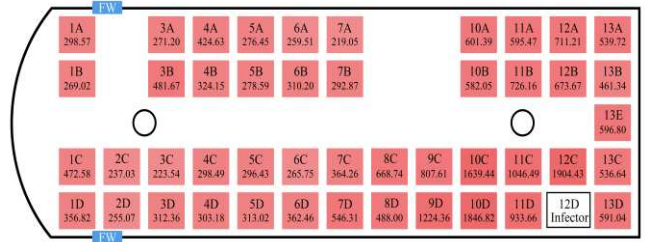
Fig. 6 (a) Temporal variation of droplet evaporation under different ambient temperature; (b) spatial distribution of droplets under various ambient temperature when no window is open. (Bus speed = 60 km/h,  $d_p = 50 \mu\text{m}$ )

Intake fraction of tracer gas

Case 1 (No windows open)  
Exposure time = 30 min

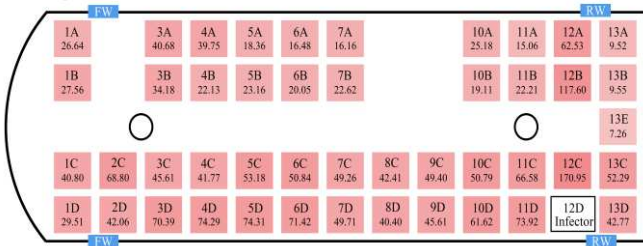


Case 2 (Only FW open)  
Exposure time = 30 min



Note: 'FW' means 'front windows'.

Case 4 (FW + RW open)  
Exposure time = 30 min



Note: 'FW' means 'front windows', 'RW' means 'rear windows'.

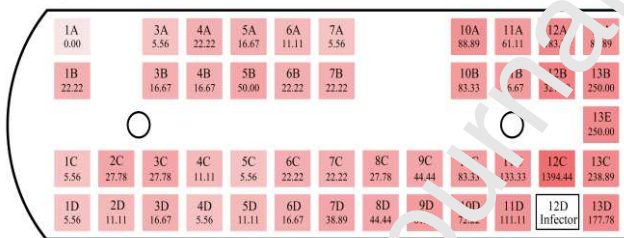
Case 6 (All windows open)  
Exposure time = 30 min



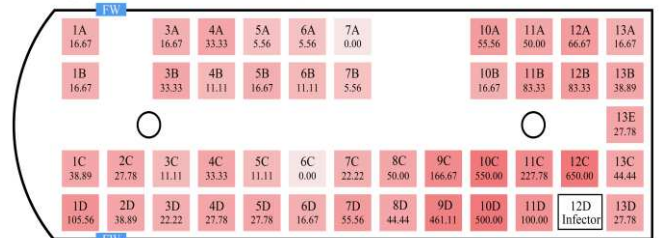
Note: 'FW' means 'front windows', 'MW' means 'middle windows', 'RW' means 'rear windows'.

Intake fraction of droplets

Case 1 (No windows open)  
Exposure time = 30 min  $d_p = 5 \mu m$

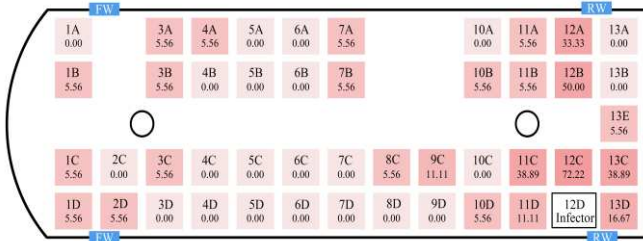


Case 2 (Only FW open)  
Exposure time = 30 min  $d_p = 5 \mu m$



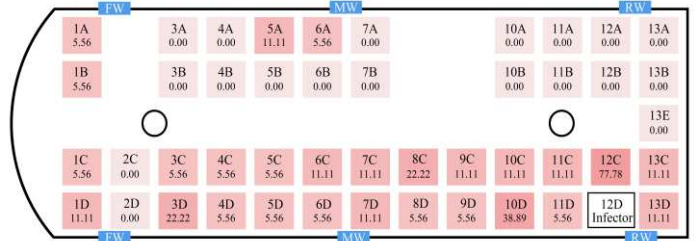
Note: 'FW' means 'front windows'.

Case 4 (FW + RW open)  
Exposure time = 30 min  $d_p = 5 \mu m$



Note: 'FW' means 'front windows', 'RW' means 'rear windows'.

Case 6 (All windows open)  
Exposure time = 30 min  $d_p = 5 \mu m$



Note: 'FW' means 'front windows', 'MW' means 'middle windows', 'RW' means 'rear windows'.

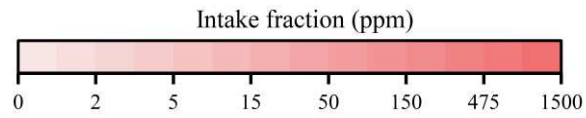
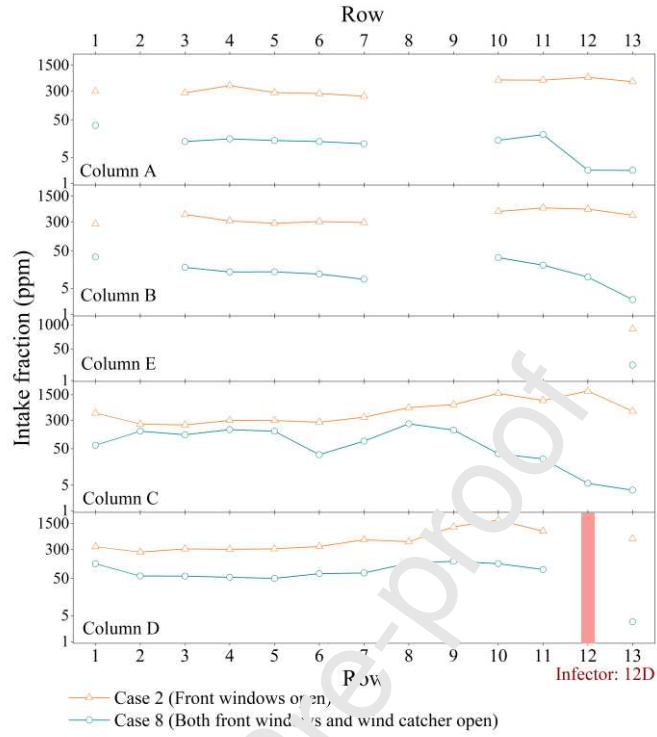


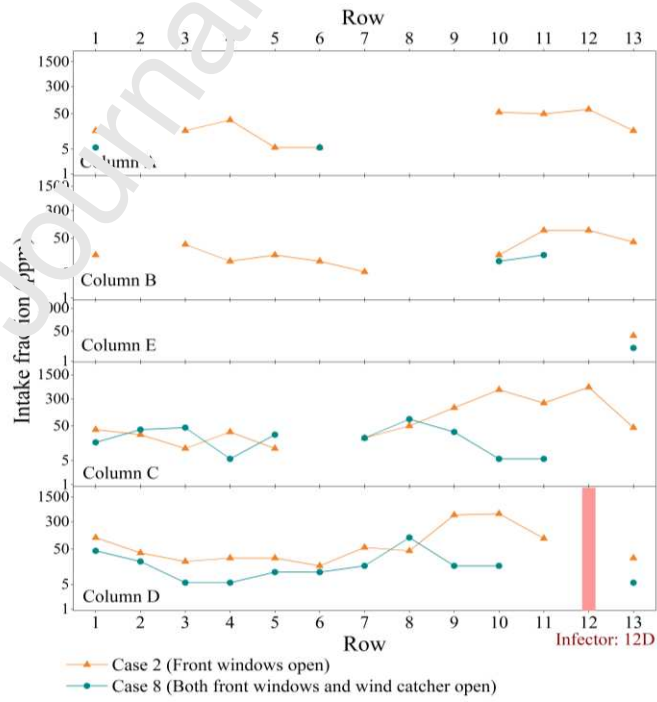
Fig. 7 Intake fraction of tracer gas and droplets under various open window configurations. (Case 6, Bus speed = 60 km/h, ambient temperature = 27 °C,  $d_p = 5$   $\mu\text{m}$ )

Journal Pre-proof

Intake fraction of tracer gas



Intake fraction of droplets



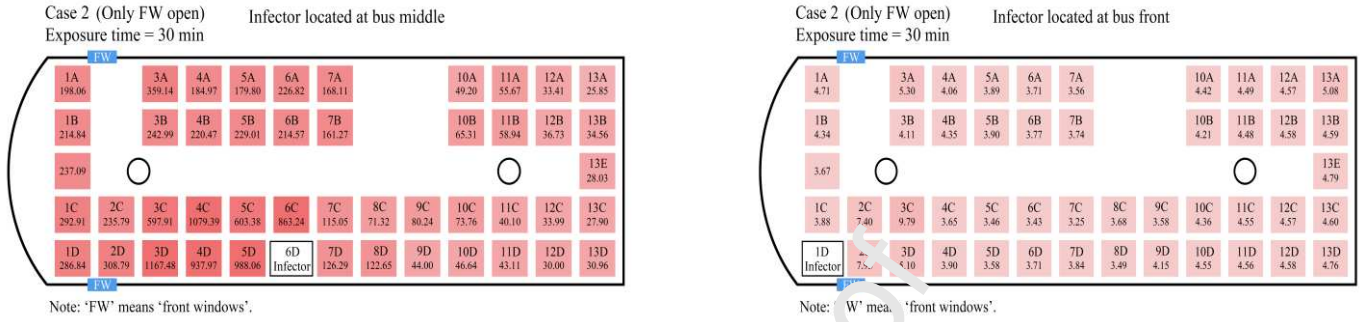
---

Fig. 8 Comparison of intake fraction with and without wind catcher when only front windows are open. (Bus speed = 60 km/h, ambient temperature = 27 °C,  $d_p = 5$   $\mu\text{m}$ )

Journal Pre-proof



Intake fraction of tracer gas



Intake fraction of droplets

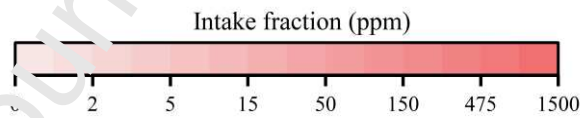
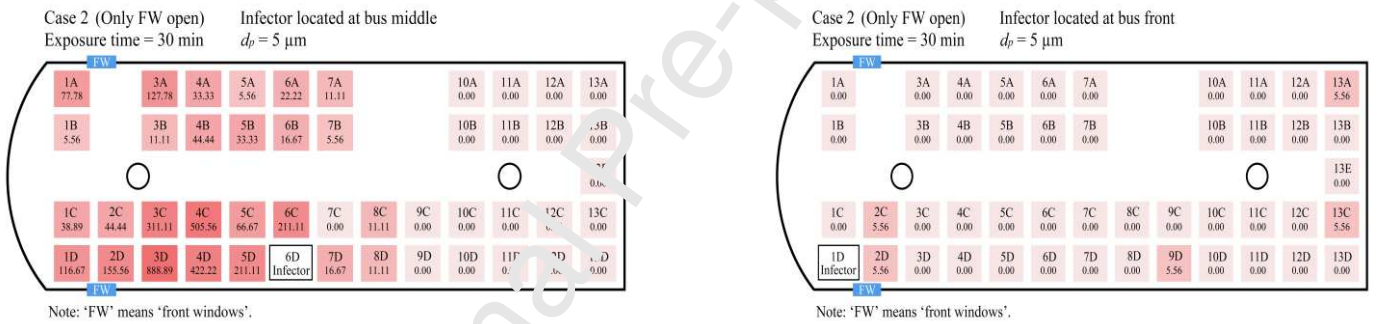
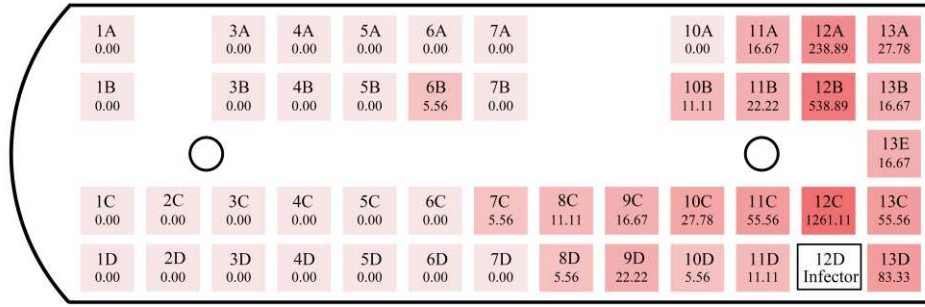


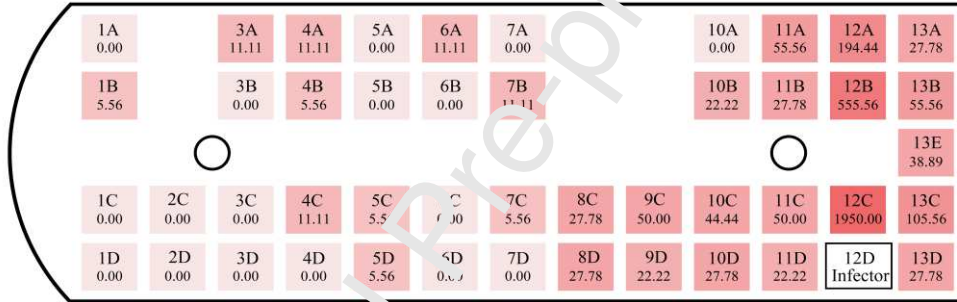
Fig. 9 Intake fraction of tracer gas and droplets under various infector's locations when only front windows are open. (Bus speed = 60 km/h, ambient temperature = 27 °C,  $d_p = 5 \mu m$ )

Case 1 (No windows open) Ambient temperature = 11 °C  
 Exposure time = 30 min  $d_p = 50 \mu\text{m}$



(a)

Case 1 (No windows open) Ambient temperature = 27 °C  
 Exposure time = 30 min  $d_p = 50 \mu\text{m}$



(b)

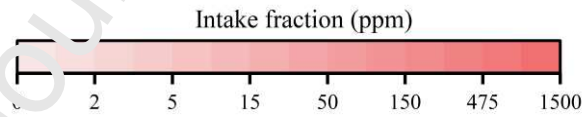
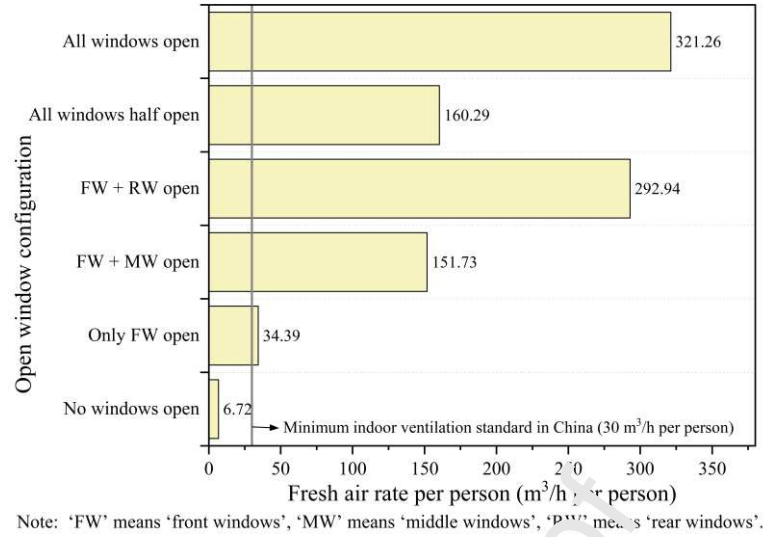
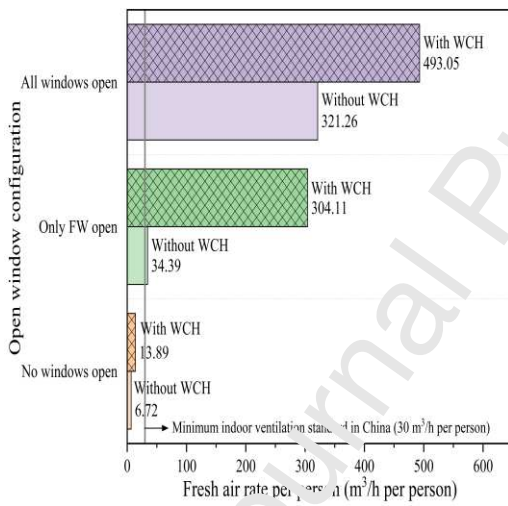


Fig. 10 Intake fraction of 50  $\mu\text{m}$  droplets when ambient temperature is (a) 11 °C; (b) 27 °C. (Bus speed = 60 km/h,  $d_p = 50 \mu\text{m}$ , no windows open)

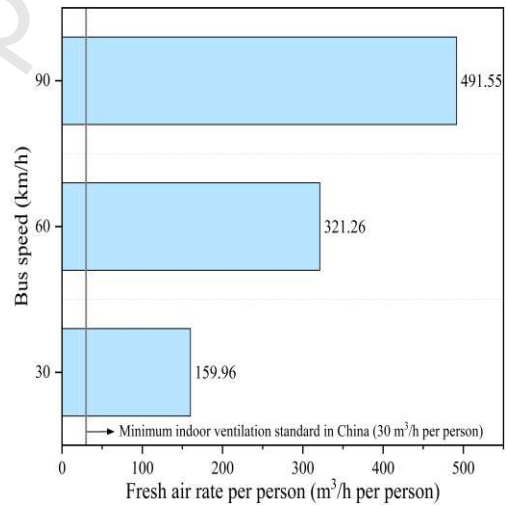




(a)



(b)



(c)

Fig. 11 Fresh air rate per person under (a) different open window configurations when bus speed is 60 km/h; (b) with and without wind catcher when bus speed is 60 km/h; (c) different bus speeds when all windows are open.




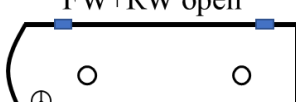
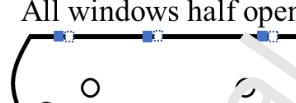
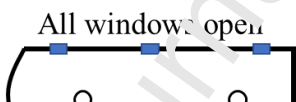
Table 1. Parameters and setups for CFD simulations.

Parameter	Open windows	Wind catcher	Speed	Temperature	Infection location
Open windows	No windows	Close	60 km/h	27 °C	Bus rear
	Only FW open	Close	60 km/h	27 °C	Bus rear
	FW + MW open	Close	60 km/h	27 °C	Bus rear
	FW + RW open	Close	60 km/h	27 °C	Bus rear
	All windows half open	Close	60 km/h	27 °C	Bus rear
	All windows open	Close	60 km/h	27 °C	Bus rear
Wind catcher	No windows	Open	60 km/h	27 °C	Bus rear

	Only	FW	Open	6	27 °C	Bus
	open			0 km/h		rear
	All windows		Open	6	27 °C	Bus
	open			0 km/h		rear
Speed	All windows		Close	3	27 °C	Bus
	open	d		0 km/h		rear
	All windows		Close	5	27 °C	Bus
	open	d		0 km/h		rear
Temper	No windows		Close	6	11 °C	Bus
ature	open	d		0 km/h		rear
Infector	Only	FW	Close	6	27 °C	Bus
location	open	d		0 km/h		middle
	Only	FW	Close	6	27 °C	Bus
	open	d		0 km/h		front

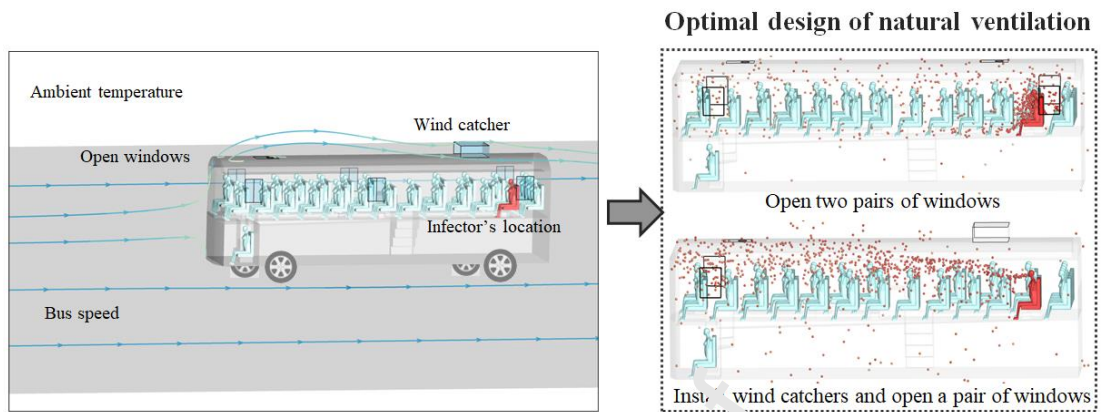
Note: 'FW' means 'front windows', 'MW' means 'middle windows', 'RW' means 'rear windows'.

Table 2. Natural ventilation under different open window configurations.

C	Open window configuration	$Q$ ( $\text{m}^3/\text{s}$ )	$ACH$ ( $\text{h}^{-1}$ )	Age of air (s)
1	No windows open 	0.09	6.14	469.03
2	Only FW open 	0.44	31.40	150.71
3	FW+MW open 	1.96	138.55	33.88
4	FW+RW open 	3.82	267.50	9.16
5	All windows half open 	2.09	146.37	15.50
6	All windows open 	4.19	293.36	8.63

Note: '⊗' means 'driver', '○' means 'skylight', '■' means 'windows', 'FW' means 'front windows', 'MW' means 'middle windows', 'RW' means 'rear windows'.

Graphical abstract



---

## Highlights

- Use coupled approach to study natural ventilation in a bus with a COVID-19 outbreak.
  
- Opening front and rear windows boosts *ACH* by 44 times and drops infection risk by 2 orders.
  
- Using a wind catcher can increase *ACH* by 8.8 times and passenger thermal comfort.
  
- Higher ambient temperature makes 50 $\mu$ m droplets suspend more and spread further.
  
- The infector's row and the three rows in front of the infector are high-risk areas.